Journal of
Nanoscience and Nanotechnology
Vol. 10, 3739–3758, 2010

Chemical Vapor Deposition of Carbon Nanotubes: A Review on Growth Mechanism and Mass Production

Mukul Kumar* and Yoshinori Ando

Department of Materials Science and Engineering, Meijo University, Nagoya 468-8502, Japan

This review article deals with the growth mechanism and mass production of carbon nanotubes (CNTs) by chemical vapor deposition (CVD). Different aspects of CNT synthesis and growth mechanism are reviewed in the light of latest progresses and understandings in the field. Materials aspects such as the roles of hydrocarbon, catalyst and catalyst support are discussed. Many new catalysts and new carbon sources are described. Growth-control aspects such as the effects of temperature, vapor pressure and catalyst concentration on CNT diameter distribution and single- or multi-wall formation are explained. Latest reports of metal-catalyst-free CNT growth are considered. The mass-production aspect is discussed from the perspective of a sustainable CNT technology. Existing problems and challenges of the process are addressed with future directions.

Keywords: Chemical Vapor Deposition (CVD), Carbon Nanotube (CNT), CNT Growth Mechanism, CNT Mass Production, CNT Industrial Production, CNT Precursor, CNT Catalyst, Catalyst-Free CNT Synthesis, Camphor.

REVIEW

CONTENTS

1. INTRODUCTION

A carbon nanotube (CNT) is a tubular structure made of carbon atoms, having diameter of nanometer order but length in micrometers. Although this kind of structures was synthesized, studied and reported by several researchers during 1952–1989,[1–17] Iijima's detailed analysis of helical arrangement of carbon atoms on seamless coaxial cylinders in 1991, proved to be a discovery report.[18] Since then, CNT has remained an exciting material ever. Its so-called extraordinary properties: many-fold stronger than steel, harder than diamond, electrical conductivity higher than copper, thermal conductivity higher than diamond, etc. set off a gold rush in academic and industrial laboratories all over the world to find practical uses of CNTs. This sprouted thousands of publications and patents on innumerous potential applications of CNTs in almost all the walks of life: media, entertainment, communication, transport, health and environment. The gold rush turned into a stampede when NASA scientists and many others predicted the possibility of making space elevators, lighter and stronger aircrafts, collapsible and reshapable cars, incredible new fabric, portable X-ray machines etc.

*Author to whom correspondence should be addressed.
E-mail: mukul@meijo-u.ac.jp

by using CNTs. Consequently, CNT has become a material of common interest today; and society is eagerly waiting for seeing the charisma of CNT in household products. However, even after 18 years of continued efforts worldwide, such products are still waitlisted.

The bottleneck is insufficient production and uncompetitive cost of CNTs with respect to the prevalent technology. Despite a huge progress in CNT research over the years, we are still unable to produce CNTs of well-defined properties in large quantities with a cost-effective technique. The root of this problem is the lack of proper understanding of the CNT growth mechanism. Till date no definitive model could be robustly established for the CNT growth. There are several issues in the growth mechanism that are yet to be clarified. Ironically, from the window of time machine, the CNT research today is ahead of its time. We, the CNT researchers, know how to make single-electron transistors from individual CNTs, but we do not know how to make a CNT of the required structure. Hence it is necessary to retrospect. The skytower of the ambitious nanotechnology (in particular, CNT-based technology) cannot be erected without a firm foundation of the growth-mechanism understanding.

Among several techniques of CNT synthesis available today, chemical vapor deposition (CVD) is most popular and widely used because of its low set-up cost, high production yield, and ease of scale-up. This review, therefore, deals with the growth mechanism and mass production of CNTs by CVD. Beginning with a brief historical account of CVD pertinent to CNT, we will cover different aspects of CNT synthesis and growth mechanism in the light of latest progresses and understandings in the field. On the materials aspect, the roles of hydrocarbon and catalyst are discussed in detail. Many new catalysts and new carbon sources are addressed. Among the new CNT precursors, camphor is highlighted because of its environment-friendliness and exceptionally-high efficiency toward CNT production. On the growth-control aspect, the effects of temperature, vapor pressure and catalyst concentration on diameter distribution and single- or multi-wall formation are discussed. The mass-production aspect is covered stressing the need of a sustainable CNT technology. Finally, we conclude with a brief mention of existing challenges and future directions.

REVIEW

2. CHEMICAL VAPOR DEPOSITION (CVD)

Chemical vapor deposition (CVD) is the most popular method of producing CNTs nowadays. In this process, thermal decomposition of a hydrocarbon vapor is achieved in the presence of a metal catalyst. Hence, it is also known as thermal CVD or catalytic CVD (to distinguish it from many other kinds of CVD used for various purposes).

2.1. History of CVD

The history of CVD for the synthesis of carbon filaments dates back to nineteenth century. In 1890, French scientists observed the formation of carbon filaments during experiments involving the passage of cyanogens over red-hot porcelain.[19] By mid-twentieth century, CVD was an established method for producing carbon microfibers utilizing

Dr. Mukul Kumar received his B.Sc., M.Sc. and Ph.D. degrees in the Faculty of Science (Physics) from Bihar University, India. During 1990–1996, he served as a Lecturer of Physics in Jai Prakash University, India. In 1996, he joined Indian Institute of Technology, Bombay and worked for Indo-French, UNESCO, DMSRDE and CSIR Projects. In Dec 2000, he joined Meijo University as a JSPS Fellow, and since Jan 2003, he has been a senior scientist at the 21st Century Centre of Excellence there. Actively involved in research, research guidance and education, Dr. Kumar's areas of interest include electrochemistry and photo-electrochemistry of group II–VI semiconductors, synthesis, characterization and application of CNTs grown by CVD method, and electron field emission. He has published 48 research articles and 6 patents on syntheses of glassy carbon and carbon nanotubes, and presented 80 papers at international conferences.

Professor Yoshinori Ando received his B.E., M.E. and D.E. degrees in the Faculty of Engineering (Applied Physics) from Nagoya University, Japan. After five years post-doctoral experience in Nagoya University, he moved to Meijo University as a Lecturer in Physics in 1974. He became Assistant Professor in 1977, and Professor in 1990. During 1987–1988, he was a visiting research fellow at Bristol University, UK. During 2000–2004, he was the first Head of the Department of Materials Science and Engineering in Meijo University. From April 2009, he is the Dean of the Faculty of Science and Technology in Meijo University. Professor Ando's research areas include X-ray diffraction topography of distorted crystals, electron microscopy of thin films and ultrafine particles of SiC, arc-discharge synthesis of CNTs and their application to composite materials. He has published over 200 research articles and a dozen of patents. He has presented over 100 papers at various conferences.

thermal decomposition of hydrocarbons in the presence of metal catalysts. In 1952 Radushkevich and Lukyanovich published a range of electron micrographs clearly exhibiting tubular carbon filaments of 50–100 nm diameter grown from thermal decomposition of carbon monoxide on iron catalyst at 600 °C.[1] They observed iron carbides encapsulated in the filament tips; accordingly, they proposed that, at first, carbon dissolution in iron resulted in the formation of iron carbide, and then, subsequent carbon deposition over iron carbide led to the formation of graphene layers. In the same year, another Russian group, Tesner and Echeistova, also reported similar carbon threads on lampblack particles exposed to methane, benzene or cyclohexane atmospheres at temperatures above 977 °C.[2] In 1953, Davis et al. published detailed electron micrographs and XRD spectra of carbon nanofibers grown from the reaction of CO and Fe_2O_4 at 450 °C in blast furnace brickworks.[3] They postulated that the catalyst for the reaction, either iron or iron carbide, formed on the surface of the iron oxide as a speck which in turn gave rise to a thread of carbon. They suggested that, at the time of carbon deposition, the catalyst particles were located on the growing ends of the threads. The threads were described as layered carbon, varying in thickness from 10 to 200 nm. Similar findings were reported by Hofer et al. (1955),[4] Walker (1959)[5] and Baird et al. (1971).[6, 7] In the 1970s extensive works were carried out independently by Baker and Endo to synthesize and understand tubular nanofibers of multi-layered carbon.[8–12] Thus, today's most-popular CNT technique, the CVD, may probably be the most-ancient technique of growing CNTs in the name of filaments and fibers. More detailed reviews of the early works have been written by Baker,[13, 14] Endo,[15, 20] and Dresselhaus.[16, 17]

2.2. Advantages of CVD

As compared to arc-discharge and laser-ablation methods, CVD is a simple and economic technique for synthesizing CNTs at low temperature and ambient pressure. In crystallinity, arc- and laser-grown CNTs are superior to the CVD-grown ones (although CVD-grown MWCNTs possess inferior crystallinity, the crystallinity of SWCNTs grown by CVD is close to that grown by arc or laser methods). However, in yield and purity, CVD beats the arc and laser methods. And, when it comes to structure control or CNT architecture, CVD is the only answer. CVD is versatile in the sense that it offers harnessing plenty of hydrocarbons in any state (solid, liquid or gas), enables the use of various substrates, and allows CNT growth in a variety of forms, such as powder, thin or thick films, aligned or entangled, straight or coiled nanotubes, or a desired architecture of nanotubes on predefined sites of a patterned substrate. It also offers better control on the growth parameters.

3. CNT SYNTHESIS

Figure 1 shows a schematic diagram of the experimental set-up used for CNT growth by CVD method in its simplest form. The process involves passing a hydrocarbon vapor (typically 15–60 min) through a tubular reactor in which a catalyst material is present at sufficiently high temperature (600–1200 °C) to decompose the hydrocarbon. CNTs grow on the catalyst in the reactor, which are collected upon cooling the system to room temperature. In the case of a liquid hydrocarbon (benzene, alcohol, etc.), the liquid is heated in a flask and an inert gas is purged through it, which in turn carries the hydrocarbon vapor into the reaction zone. If a solid hydrocarbon is to be used as the CNT precursor, it can be directly kept in the low-temperature zone of the reaction tube. Volatile materials (camphor, naphthalene, ferrocence etc.) directly turn from solid to vapor, and perform CVD while passing over the catalyst kept in the high-temperature zone. Like the CNT precursors, also the catalyst precursors in CVD may be used in any form: solid, liquid or gas, which may be suitably placed inside the reactor or fed from outside. Pyrolysis of the catalyst vapor at a suitable temperature liberates metal nanoparticles *in-situ* (such a process is known as floating catalyst method). Alternatively, catalyst-coated substrates can be placed in the hot zone of the furnace to catalyze the CNT growth.

CNT growth mechanism has been debatable right from its discovery. Based on the reaction conditions and post-deposition product analyses, several groups have proposed several possibilities which are often contradicting. Therefore, no single CNT growth mechanism is well established till date. Nevertheless, widely-accepted most-general mechanism can be outlined as follows. Hydrocarbon vapor when comes in contact with the "hot" metal nanoparticles, first decomposes into carbon and hydrogen species; hydrogen flies away and carbon gets dissolved into the metal. After reaching the carbon-solubility limit in the metal at that temperature, as-dissolved carbon precipitates out and crystallizes in the form of a cylindrical network having no dangling bonds and hence energetically stable. Hydrocarbon decomposition (being an exothermic process) releases some heat to the metal's exposed

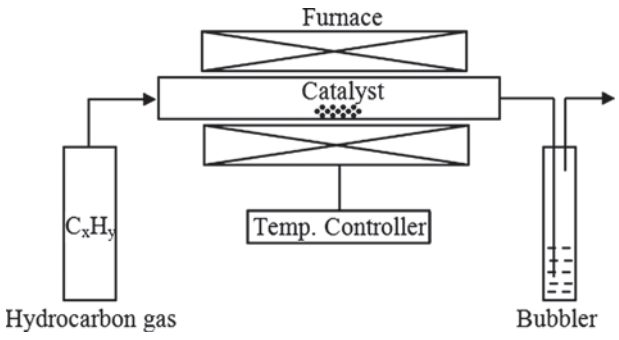

Fig. 1. Schematic diagram of a CVD setup in its simplest form.

zone, while carbon crystallization (being an endothermic process) absorbs some heat from the metal's precipitation zone. This precise thermal gradient inside the metal particle keeps the process on.

Now there are two general cases. (Fig. 2(a)) When the catalyst–substrate interaction is weak (metal has an acute contact angle with the substrate), hydrocarbon decomposes on the top surface of the metal, carbon diffuses down through the metal, and CNT precipitates out across the metal bottom, pushing the whole metal particle off the substrate (as depicted in step (i)). As long as the metal's top is open for fresh hydrocarbon decomposition (concentration gradient exists in the metal allowing carbon diffusion), CNT continues to grow longer and longer (ii). Once the metal is fully covered with excess carbon, its catalytic activity ceases and the CNT growth is stopped (iii). This is known as "tip-growth model."[8]

In the other case, (Fig. 2(b)) when the catalyst–substrate interaction is strong (metal has an obtuse contact angle with the substrate), initial hydrocarbon decomposition and carbon diffusion take place similar to that in the tip-growth case, but the CNT precipitation fails to push the metal particle up; so the precipitation is compelled to emerge out from the metal's apex (farthest from the substrate, having minimum interaction with the substrate). First, carbon crystallizes out as a hemispherical dome (the most favorable closed-carbon network on a spherical nanoparticle) which then extends up in the form of seamless graphitic cylinder. Subsequent hydrocarbon deposition takes place on the lower peripheral surface of the metal, and as-dissolved carbon diffuses upward. Thus CNT grows up with the catalyst particle rooted on its base; hence, this is known as "base-growth model."[10]

Formation of single- or multi-wall CNT (SWCNT or MWCNT, respectively) is governed by the size of the catalyst particle.[21] Broadly speaking, when the particle size is a few nm, SWCNT forms; whereas particles—a few tens nm wide—favor MWCNT formation. With such an approximate growth picture in mind, we can proceed to other important aspects of the CNT growth. Detailed discussion on the growth mechanism is presented in Section 5.

CNT synthesis involves many parameters such as hydrocarbon, catalyst, temperature, pressure, gas-flow rate, deposition time, reactor geometry. However, to keep our discussion compact, here we will consider only the three key parameters: hydrocarbon, catalyst and catalyst support.

3.1. CNT Precursors

Most commonly used CNT precursors are methane,[22,23] ethylene,[24,25] acetylene,[26] benzene,[27] xylene,[28] and carbon monoxide.[29] Endo et al.[30–32] reported CNT growth from pyrolysis of benzene at 1100 °C, whereas Jose-Yacaman et al.[33] got clear helical MWCNTs at 700 °C from acetylene. In those cases iron nanoparticles were used as the catalyst. Later, MWCNTs were also grown

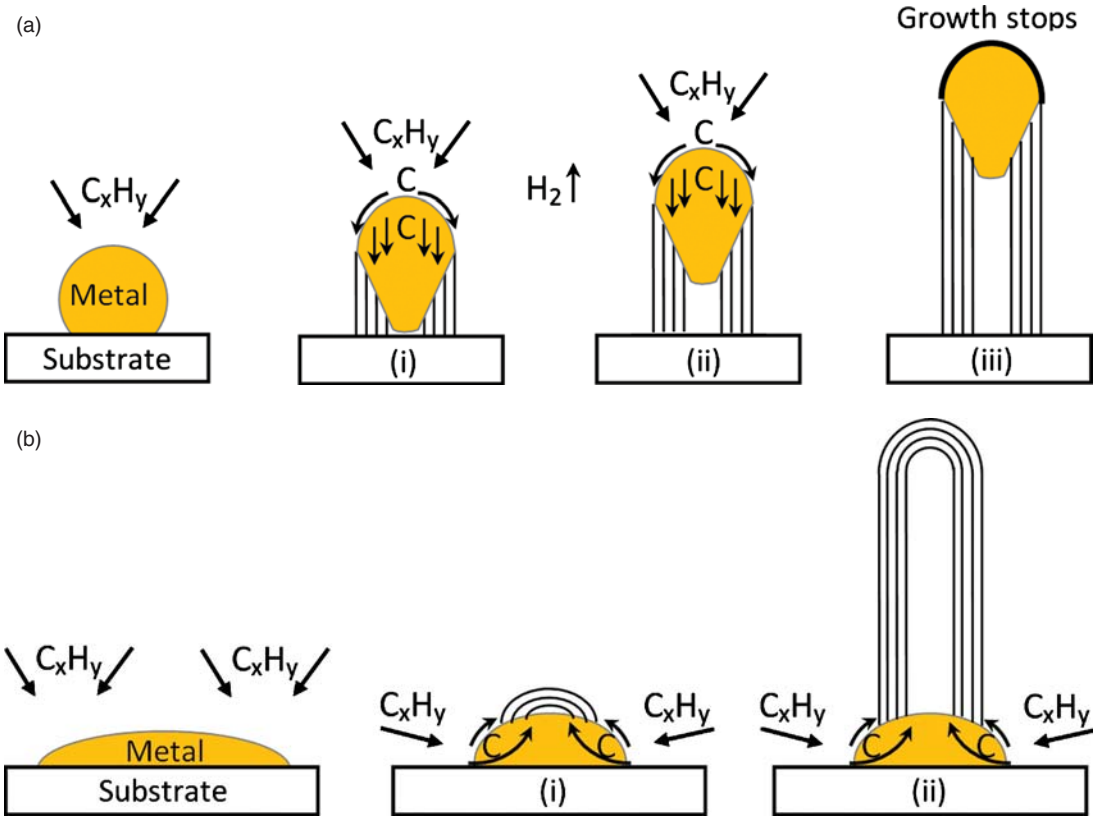

Fig. 2. Widely-accepted growth mechanisms for CNTs: (a) tip-growth model, (b) base-growth model.

from many other precursors including cyclohexane,[34, 35] and fullerene.[36, 37] On the other hand, SWCNTs were first produced by Dai et al.[38] from disproportionation of carbon monoxide at 1200 °C, in the presence of molybdenum nanoparticles. Later, SWCNTs were also produced from benzene,[39] acetylene,[40] ethylene,[41] methane,[23, 42] cyclohexane,[43] fullerene[44] etc. by using various catalysts. In 2002 Maruyama et al. reported the low-temperature synthesis of high-purity SWCNTs from alcohol on Fe–Co-impregnated zeolite support;[45] and since then, ethanol became the most popular CNT precursor in the CVD method worldwide.[46–48] Special feature of ethanol is that ethanol-grown CNTs are almost free from amorphous carbon, owing to the etching effect of OH radical.[49] Later, vertically-aligned SWCNTs were also grown on Mo-Co-coated quartz and silicon substrates.[50, 51] Recently, Maruyama's group has shown that intermittent supply of acetylene in ethanol CVD significantly assists ethanol in preserving the catalyst's activity and thus enhances the CNT growth rate.[52]

The molecular structure of the precursor has a detrimental effect on the morphology of the CNTs grown. Linear hydrocarbons such as methane, ethylene, acetylene, thermally decompose into atomic carbons or linear dimers/trimers of carbon, and generally produce straight hollow CNTs. On the other hand, cyclic hydrocarbons such as benzene, xylene, cyclohexane, fullerene, produce relatively curved/hunched CNTs with the tube walls often bridged inside.[36, 37]

General experience is that low-temperature CVD (600–900 °C) yields MWCNTs, whereas high-temperature (900–1200 °C) reaction favors SWCNT growth. This indicates that SWCNTs have a higher energy of formation (presumably owing to small diameters; high curvature bears high strain energy). Perhaps that is why MWCNTs are easier to grow (than SWCNTs) from most of the hydrocarbons, while SWCNTs grow from selected hydrocarbons (viz. carbon monoxide, methane, etc. which have a reasonable stability in the temperature range of 900–1200 °C). Commonly efficient precursors of MWCNTs (viz. acetylene, benzene, etc.) are unstable at higher temperature and lead to the deposition of large amounts of carbonaceous compounds other than the nanotubes.

In 2004, using ethylene CVD, Hata et al. reported water-assisted highly-efficient synthesis of impurity-free SWCNTs on Si substrates.[53] They proposed that controlled supply of steam into the CVD reactor acted as a weak oxidizer and selectively removed amorphous carbon without damaging the growing CNTs. Balancing the relative levels of ethylene and water was crucial to maximize the catalyst's lifetime. However, very recently, Zhong et al. have shown that a reactive etchant such as water or hydroxyl radical is not required at all in cold-wall CVD reactors if the hydrocarbon activity is low.[54] These studies emphatically prove that the carbon precursor plays a crucial role in CNT growth. Therefore, by proper selection of CNT precursor and its vapour pressure, both the catalyst's lifetime and the CNT-growth rate can be significantly increased; and consequently, both the yield and the quality of CNTs can be improved.

3.2. CNT Catalysts

For synthesizing CNTs, typically, nanometer-size metal particles are required to enable hydrocarbon decomposition at a lower temperature than the spontaneous decomposition temperature of the hydrocarbon. Most commonly-used metals are Fe, Co, Ni, because of two main reasons: (i) high solubility of carbon in these metals at high temperatures; and (ii) high carbon diffusion rate in these metals. Besides that, high melting point and low equilibrium-vapor pressure of these metals offer a wide temperature window of CVD for a wide range of carbon precursors. Recent considerations are that Fe, Co, and Ni have stronger adhesion with the growing CNTs (than other transition metals do) and hence they are more efficient in forming high-curvature (low-diameter) CNTs such as SWCNTs.[55]

Solid organometallocenes (ferrocene, cobaltocene, nickelocene) are also widely used as a CNT catalyst, because they liberate metal nanoparticles *in-situ* which catalyze the hydrocarbon decomposition more efficiently. It is a general experience that the catalyst-particle size dictates the tube diameter. Campbell's group has reported the particle-size dependence and a model for iron-catalyzed growth of CNTs.[37] Hence, metal nanoparticles of controlled size, pre-synthesized by other reliable techniques, can be used to grow CNTs of controlled diameter.[56] Thin films of catalyst coated on various substrates are also proven good in getting uniform CNT deposits.[24] The key factor to get pure CNTs is achieving hydrocarbon decomposition on the catalyst surface alone, and prohibiting the aerial pyrolysis.

Apart from the popular transition metals (Fe, Co, Ni), other metals of this group, such as Cu, Au, Ag, Pt, Pd were also found to catalyze various hydrocarbons for CNT growth. A comprehensive review of the role of metal particles in the catalytic growth of CNTs has been published by Kauppinen's group.[57]

On the role of CNT catalysts, it is worth mentioning that transition metals are proven to be efficient catalysts not only in CVD but also in arc-discharge and laser-vaporization methods. Therefore, it is likely that these apparently different methods might inherit a common growth mechanism of CNT, which is not yet clear. Hence this is an open field of research to correlate different CNT techniques in terms of the catalyst's role in entirely different temperature and pressure range.

3.3. CNT Catalyst Supports

The same catalyst works differently on different support materials. Commonly used substrates in CVD are graphite,[8, 9] quartz,[58, 59] silicon,[53, 60] silicon carbide,[61, 62]

silica,[63, 64] alumina,[65, 66] alumino-silicate (zeolite),[67, 68] $CaCO_3$,[69] magnesium oxide,[70–72] etc. For an efficient CNT growth, the catalyst–substrate interaction should be investigated with utmost attention. Metal–substrate reaction (chemical bond formation) would cease the catalytic behavior of the metal. The substrate material, its surface morphology and textural properties greatly affect the yield and quality of the resulting CNTs. Zeolite supports with catalysts in their nanopores have resulted significantly high yields of CNTs with a narrow diameter distribution.[68, 73] Alumina materials are reported to be a better catalyst support than silica owing to the strong metal–support interaction in the former, which allows high metal dispersion and thus a high density of catalytic sites.[74] Such interactions prevent metal species from aggregating and forming unwanted large clusters that lead to graphite particles or defective MWCNTs.[75] Recent *in-situ* XPS analysis of CNT growth from different precursors on iron catalyst supported on alumina and silica substrates have confirmed these theoretical assumptions.[64] Thin Alumina flakes (0.04–4 μm thick) loaded with iron nanoparticles have shown high yields of aligned CNTs of high aspect ratio.[76] Latest considerations are that the oxide substrate, basically used as a physical support for the metal catalyst, might be playing some chemistry in the CNT growth.[77] Acoordingly, the chemical state and structure of the substrate are more important than that of the metal.

3.4. New (Uncommon) CNT Catalysts

Recent developments in the nanomaterials synthesis and characterization have enabled many new catalysts for the CNT growth. Apart from popularly used transition metals (Fe, Co, Ni), a range of other metals (Cu, Pt, Pd, Mn, Mo, Cr, Sn, Au, Mg, Al) has also been successfully used for horizontally-aligned SWCNT growth on quartz substrates.[78] Unlike transition metals, noble metals (Au, Ag, Pt, Pd etc.) have extremely low solubility for carbon, but they can dissolve carbon effectively for CNT growth when their particle size is very small (<5 nm).[79, 80] Daisuke et al. have succeeded in controlled growth of SWCNTs on Au nanoparticles deposited on atomic steps of Si. It has been proposed that the active catalyst is Au–Si alloy with about 80 at% Au.[71]

Although copper is a transition metal, it showed insignificant catalytic effect on the CNT growth in the past.[82–85] In fact, it had been considered as an adverse contaminant. As a recent development, however, it has been found to catalyze the CNT growth efficiently. Methane and ethanol decomposition at 825–925 °C on Cu nanoparticles supported on silicon wafers produced high densities of well-crystallined SWCNTs up to 1 cm in length.[86] The Cu nanoparticles were synthesized by the reduction of $CuCl_2$ in the presence of Cu_2O nanoparticles produced by the thermolysis of cupric formates in coordinating solvents.[87] This implies that the novelty lies in the catalyst-preparation method.

Rhenium (Re) is a rare catalyst used for CNT growth. Diamagnetic SWCNTs and MWCNTs were reported by methane decomposition on Re catalyst.[88] The current scenario is that, just as any carbon-containing material can yield CNT, any metal can catalyze the CNT growth, provided that the experimental conditions are properly optimized.

3.5. Metal-Free CNT Growth

Very recently nanodiamond particles (5 nm) were successfully used as a CNT catalyst. Ethanol suspension of nanodiamond particles was spread on graphite plates and dried in air at 600 °C. This resulted in isolated diamond particles, monolayers of diamond, and multilayered-diamond stacks on the substrate, depending upon the diamond concentration (0.01–1.0 wt%). Ethanol CVD over these diamond-loaded substrates at 850 °C produced isolated CNTs, layered CNTs and high-density CNT mats, respectively. The nanodiamond particles do not fuse even after high-temperature CVD process, implying that they remain in solid state during CVD. Nanodiamond is therefore said to act as a CNT growth seed.[89] This result proves that CNT growth is possible without metal catalyst. Does nanodiamond act as a catalyst? If it does, how? These are open questions.

In many studies, oxygen was noticed to activate the CNT growth. Recent studies have revealed that many metals, which do not exhibit catalytic activity in pure-metal form, do well in oxide form.[90] Does metal oxide act as a catalyst? Template-free directional growth of CNTs has been achieved on sapphire.[91] CNTs have also been grown on semiconductors such as Si and Ge nanoparticles (though C has little solubility in bulk Si or Ge), provided that the nanoparticles are heated in air just before CVD.[92] Similarly, CNT growth on SiC substrates takes place only when some oxygen is present in the chamber.[93] Porous Al_2O_3 has already been shown to facilitate CNT growth without any catalyst.[94, 95] Catalyst-free CNT growth is also possible in oxy-fuel flames.[96] And oxide, typically used as a catalyst support in CVD, is itself capable of forming graphene layers.[97] All these examples resoundingly indicate that oxygen plays a key role in CNT growth. The question is: is it a catalyst? HRTEM investigation of the CNTs grown by cyclohexane pyrolysis over iron nanoparticles supported on thin Al_2O_3 layers shows that CNT keeps on growing even when the metal is completely encapsulated in the tube center.[98] The authors propose that the metal only helps to initiate the CNT precipitation at the nucleation stage. Once the CNT head is created, metal becomes non functional; subsequent carbon addition to the CNT base periphery is facilitated by the substrate's oxide layer. This concept is radically different to the existing concept that the metal must remain exposed (either on the CNT tip or base) to keep the growth on. Hence more careful *in-situ* observation

and robust theoretical support are required to establish the oxide's direct role as a catalyst.

The latest development of the field is even more exciting. CNT growth is possible with no metal at all; the non-metallic substrate itself acts as the catalyst. Liu et al. passed methane and hydrogen (1:1) over an SiO_2-sputtered Si wafer at 900 °C for 20 min and got dense SWCNTs grown on it. In the same CVD condition, thermally-grown SiO_2 films did not result CNTs. The success lies in the *in-situ* transformation of the sputtered SiO_2 film (30 nm) into isolated Si particles (1.9 nm) which efficiently catalyzed methane decomposition due to small-size effect.[99] Similar SiO_2 nanoparticle generation and subsequent CNT growth was reported by Liu et al. from ethanol decomposition on annealed SiO_2/Si substrates.[100] On the other hand, Huang et al. simply scratched the existing SiO_2/Si wafers by a diamond blade and passed ethanol over it at 900 °C for 10 min.[101] Bunch of SWCNTs grew on the scratched portions. Random scratches on thin SiO_2 films protrude some nanoparticles mechanically. These developments raise many new questions and compel us to reconsider the existing CNT-growth models. SiO_2 has no carbon solubility; how does it assist hydrocarbon-to-CNT conversion? Does it act as a solid-state catalyst like nanodiamond? Or does it melt at 900 °C as usual metal nanoparticles do? If it is in molten state, Si and O atoms might have some mobility thus creating a vacancy or dislocation which would attract hydrocarbon and cause dehydrogenation. If it is in solid state, it would be strained enough (high curvature at small particle size) and could possibly interact with hydrocarbon. It is also likely that it is in a quasi-liquid (fluctuating solid) state; slight distortion in its overall shape would develop some polarity on Si and O atoms, which could possibly facilitate dehydrogenation; and its fluctuating shape could act as a template for tubular graphite formation. These speculations evoke serious discussion. SiO_2 has a number of distinct crystalline forms. Si–O bond length and Si–O–Si bond angle vary significantly in different crystal forms (e.g., 154–171 pm, 140°–180°). *Ab-initio* calculations have indicated that CNT-cap nucleation is influenced by solid-surface curvatures.[102] More theoretical considerations and experimental verifications are sought for proper understanding of CNT growth on SiO_2 nanoparticles. It will take due time to come up with a convincing model; nevertheless, there is no doubt that metal-free CNT synthesis is a major breakthrough in CNT research, and it has opened up a new avenue in nanotechnology.

3.6. New (Unconventional) CNT Precursors

Apart from the popular hydrocarbons mentioned in Section 3.1, CNTs have also been synthesized from many other organic compounds, especially from polymers. Carbonization (prolonged pyrolysis in vacuum to convert organic compounds into solid carbon) of polyacrylonitrile[103] and poly-furfuryl-alcohol[104] within nanoporous alumina templates resulted in thick CNTs. Reported in 1995–96, this was a multi-step tedious process requiring chemically-controlled monomer initiators to achieve polymerization. The field has matured enough and nowadays super-aligned highly-uniform CNTs can be produced from readily available polymers without taking pains for chemical initiators or catalysts. Recently, several polymer precursors, loaded on commercially-available alumina templates of well-defined pore size, were carbonized (400–600 °C for 3 h) to obtain MWCNTs of desired diameter.[105] N-doped MWCNTs obtained from carbonization of polypyrrole within alumina and zeolite membranes have shown better hydrogen-storage capacity than pristine MWCNTs obtained from polyphenyl acetylene in the same conditions.[106] As for SWCNT, pyrolysis of tripropylamine within the nanochannels (0.73 nm) of aluminophosphate crystals (AFI) resulted in the smallest nanotubes (0.4 nm).[107] Later, several carbon precursors were pyrolyzed within the AFI channels and tetrapropylammonium hydroxide was found to yield high densities of 4Å CNTs with better crystallinity.[108] It is suggested that the number of carbon atoms in the precursor molecule influences the SWCNT packing density in the template channels.

Among other organic compounds, amino-dichloro-s-triazine, pyrolyzed on cobalt-patterned silica substrates, resulted in highly pure CNTs.[109] Almost contemporary, organometallic compounds such as metallocene (ferrocene, cobaltocene, nickelocene)[27] and nickel phthalocyanine[110] were used as the carbon-cum-catalyst precursor; however, as-grown CNTs were highly metal-encapsulated and the yield was very low. Later, pyrolysis of thiophene with metallocene led to the formation of *Y*-junction CNTs.[111, 112] Recently, high-temperature pyrolysis (1300 °C) of simple saccharides (from table sugar (sucrose) to lactose) resulted in straight as well as helical MWCNTs.[113]

In 2001 high yield of CNTs was obtained from camphor, a tree product.[114] Since then the authors remained involved with this environment-friendly source of CNTs and established the conditions for growing MWCNTs,[115, 116] SWCNTs,[117] and vertically-aligned CNTs on quartz and silicon substrates[59, 60, 118] using ferrocene catalyst. Later, using Fe–Co catalyst impregnated in zeolite support, mass production of CNTs was achieved by camphor CVD.[68, 119] MWCNTs were grown at a temperature as low as 550 °C, whereas SWCNTs could be grown at relatively high (900 °C) temperature. Because of very low catalyst requirement with camphor, as-grown CNTs are least contaminated with metal, whereas oxygen atom present in camphor helps in oxidizing amorphous carbon *in-situ*. These features of camphor stimulated more in-depth, basic and applied research worldwide. Collaboration of India, UK and Japan reported the use of camphor-grown CNTs

as the anode of secondary lithium battery.[120] Scientists at the University of Edinburgh investigated the effect of camphor's molecular structure on the CNT growth and quality.[121] Researchers at Tokyo University of Science studied camphor CVD with different ways of catalyst feeding and addressed catalyst activation/deactivation process for the synthesis of highly-dense aligned CNT arrays.[122] Another Japanese group synthesized aligned CNTs from camphor and reported their field emission properties.[123, 124] South African scholars studied the effect of carrier gases (nitrogen, argon, argon–hydrogen mixture) as well as catalyst–support materials (SiO_2, Al_2O_3 and MgO) on the quality of camphor-grown CNTs.[125] Brazilian scientists carried out thermal annealing and electrochemical purification of camphor-grown CNTs.[126] Chinese carbon group synthesized tree-like multi-branched CNTs from camphor and reported the effects of temperature, argon flow rate and catalyst concentration on the structure of as-grown carbon nanotrees.[127] Italian carbon group investigated different aspects of camphor-CVD and published a series of reports. Musso et al. achieved low-temperature (650 °C) growth of vertically-aligned CNTs on various glass substrates and confirmed the high CNT-growth efficiency of camphor.[128] Porro et al. optimized the CNT growth parameters by Taguchi method and got 2.3 mm thick CNT mats at a high deposition rate of 500 nm/sec.[129, 130] Later, the same group published fluid-dynamic analysis of the carrier-gas flow for camphor-CVD system[131, 132] and hydrogen-storage analysis of different kinds of CNTs.[133] Thus, camphor has emerged as a promising and the most-efficient CNT precursor amongst the new/unconventional ones. Moreover, it has opened up a new avenue of exploring other botanical products as a CNT precursor. Appreciable efforts have been made in India by Sharon and his coworkers who investigated the pyrolysis of a range of plant-based materials for this purpose.[134] Recently, high yields of aligned and non-aligned CNTs have also been reported from other plant-derived cheap raw materials such as turpentine[135–137] and eucalyptus oils.[138]

Apart from the well-defined chemical reagents described above, CNTs have also been successfully and systematically synthesized from domestic fuels such as kerosene,[139] coal gas,[140] and liquefied petroleum gas.[141] More interestingly, there are scientific reports of CNT production from green grasses. Grass contains dense vascular bundles in the stem and branches. They are mainly composed of cellulose, hemicellulose and lignin. Rapid heat treatment of grass (600 °C) in controlled-oxygen ambience dehydrates and carbonizes the vascular bundles into CNTs.[142] Thus, now it is almost certain that any carbon-containing material may be a CNT precursor under suitable experimental conditions. The point is: can we reproduce the product quality and quantity from those materials of inconsistent composition? Certainly not. Depending upon the chemical composition of the raw material, one will have to change the experimental conditions every now and then; and the impurity elements of the raw material would greatly contaminate the resulting CNTs which would ultimately be of no practical importance. Hence, these novel and interesting researches of CNT production from garbage materials seem to be too long-term project. To meet the immediate need of mass production of CNTs, it is advisable to choose a raw material of consistent chemistry, which is highly abundant and regenerative too; so that it could lead to a reproducible as well as sustainable industrial technique.

4. CNT GROWTH CONTROL

It is well known that hydrocarbons are easily broken at high temperatures. Such a thermal decomposition is called Pyrolysis. However, in the presence of suitable metal catalysts, a hydrocarbon can be decomposed at lower temperatures (catalytic pyrolysis). The key of CNT growth by CVD is to achieve the hydrocarbon decomposition on the metal surface alone and prohibit spontaneous aerial pyrolysis (do not allow the hydrocarbon to break uncatalyzed, beyond the catalyst surface). Restriction of pyrolysis to the catalyst surface is controlled through proper selection of hydrocarbon and catalyst materials, vapor pressure of the hydrocarbon, concentration of the catalyst, and the CVD reaction temperature. Choosing camphor as the carbon source, the rest three key parameters were categorically optimized in our laboratory.

4.1. Effect of Catalyst Material and Concentration

Early experiments of CNTs were carried out with different metal catalysts (Fe, Co, Ni) separately. Iron was found to have high catalytic effect in hydrocarbon decomposition leading to higher CNT deposits, but those CNTs were poorly graphitized.[22] On the other hand, cobalt catalyst resulted in better-graphitized CNTs but the yield went down.[73] Hence a mixture of the two metals were tried to combine their individual advantages, and it was successful. Large volumes of well-graphitized MWCNTs were obtained. Additional advantage of using the bimetallic catalyst was that CNTs could be grown at much lower temperature viz. 550 °C. It is because the melting point of the mixture of Fe and Co is lower than their individual melting points. Moreover, alloys are known to be better catalysts than pure metals. These trends suggest that tri-metallic catalysts should also give interesting results, though the interpretation of result would be more complicated. No much effort is known in this direction.

Besides the catalyst material, the catalyst concentration also plays an important role in the CNT growth. In our lab, catalyst concentration in zeolite was varied in a wide range (1–50 wt%). No CNT formed for a catalyst concentration less than 2.4 wt% in zeolite. Lower catalyst concentrations (2.4–5%) exhibited SWCNT growth (at 850 °C and above),

whereas higher concentrations favored MWCNT growth. A combined Fe + Co concentration of 40% accounted for the highest yield of MWCNTs with negligible metal contamination.[119] These studies confirm that SWCNTs or MWCNTs can be selectively grown by proper selection of catalyst materials and their concentration.

4.2. Effect of Temperature

The authors investigated the effect of temperature on camphor CVD in a wide range of 500–1000 °C. It was noticed that camphor did not decompose below 500 °C. At 550 °C very short-length tubes emerged from the zeolite pores suggesting that the catalyst activity, and hence the CNT growth rate, was quite low at 550 °C (Fig. 3(a)). However, the CNT growth abruptly increased at 600 °C, and a profound growth was observed all around the zeolite pores (Fig. 3(b)). At 650°C and above, the growth rate was so enormous that hardly a zeolite particle could be located amid nanotubes. TEM investigations revealed that the CNT diameter increased with the increasing growth temperature. Very clean CNTs, almost free from metallic impurity, were produced up to 750 °C. This suggests that, at low temperatures, the catalyst–support interaction is strong enough not to let the metal particles leave the zeolite matrix. So, the CNTs grow via base-growth process. However, at higher temperatures, the metal particles were gradually pronounced in the samples, preferably encapsulated at the CNT tips. This suggests that, at critical temperatures, tip-growth process coexists with base-growth process, due to inhomogenity of metal dispersion. Bigger metal clusters may leave a part of it to be lifted up with the growing CNTs.

From 750 °C onward, both the diameter and the diameter-distribution range increased drastically. It is supposed that, at high temperature, the metal atoms agglomerate into bigger clusters leading to thick CNTs. Simultaneously; high temperature promotes camphor decomposition leading to more carbon generation and hence more wall formation. At 850 °C and above, SWCNTs began to form besides MWCNTs and the volume of SWCNTs increased with the increasing temperature. For instance, in 900 °C sample (Fig. 3(c)) large bundles of SWNTs can be seen (in low contrast) underneath thick fibers (in high contrast). It is noteworthy that, while MWCNTs and fibers have a lot of metal contamination, there is no trace of metal associated with the SWCNT bundles (Figs. 3(c, d)). Thus, the best temperature for a gigantic growth of MWCNTs, was found to be 650 °C, as optimized for Fe–Co-impregnated zeolite

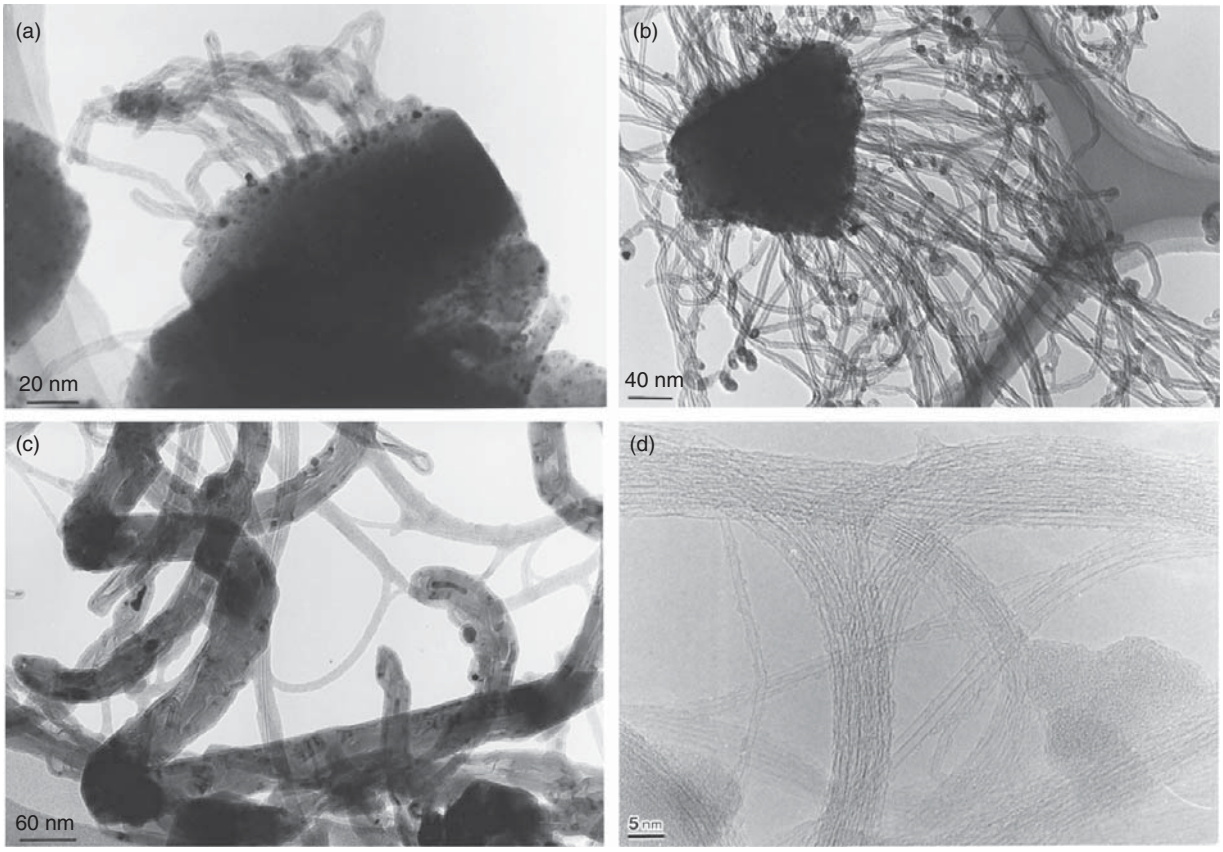

Fig. 3. TEM images of MWCNTs grown at low temperatures and atmospheric pressure: (a) 550 °C, (b) 600 °C, (c) 900 °C, (d) SWCNTs at 900 °C. Reprinted with permission from [68], M. Kumar and Y. Ando, *Carbon* 43, 533 **(2005)**. © 2005, Elsevier Science.

catalyst. CNTs grown at such a low temperature were almost free from metal particles as well as amorphous carbon. On the other hand, the best temperature for SWCNT growth from camphor on Fe–Co–zeolite system was noted to be 900 °C, restricting the total metal concentration (Fe+ Co) to 2.4 wt% in zeolite (Fig. 3(d)). In such a low concentration, the metal content remains confined to the zeolite host even at 900 °C, and does not contaminate the growing SWCNTs. Thus, the CVD temperature plays the central role in CNT growth. For a fixed metal concentration, the increasing CVD temperature increases the diameter distribution. On the other hand, MWCNTs and SWCNTs can be selectively grown as a function of CVD temperature, if the catalyst's concentration is properly optimized.[68] A good account of the effect of temperature on the growth and structure of CNTs is reported by Li et al.[143]

4.3. Effect of Vapor Pressure

For controlled growth of CNTs by CVD, the vapor pressure of the hydrocarbon in the reaction zone is another very important parameter. For gaseous hydrocarbons, a desired vapor pressure in the CVD reactor can be maintained by limited gas-flow rate and controlled suction with a rotary pump.[144] In the case of a liquid hydrocarbon, its vapor pressure is controlled by its heating temperature before it enters the reactor.[145] However, for a solid hydrocarbon such as camphor, it is quite tricky to control its vapor pressure. It becomes a function of three parameters: camphor mass, its vaporization temperature, and the flow rate of argon—the carrier gas. By proper optimization of these three parameters, the influx of camphor vapor to the zeolite bed and its decomposition rate were balanced to a great extent, and a record growth of MWCNTs was achieved at atmospheric-pressure CVD.[119] On the other hand, pure SWCNTs (free from MWCNTs) were selectively obtained from camphor CVD at low pressures (10–40 torr) where the camphor vapor pressure is quite in tune with the low metal concentration.[68] Unfortunately, however, the quantity of such pure SWCNTs is still in milligram order. Gram-order SWCNT synthesis from camphor is still an open field of research.

5. CNT GROWTH MECHANISM UNDER ELECTRON MICROSCOPY

As briefly outlined in Section 3, most widely-accepted CNT growth model assumes that the hydrocarbon vapor is adsorbed to the metal nanoparticles; and catalytically-decomposed carbon species diffuse through the metal particle, and upon reaching supersaturation, precipitate out in the form of seamless carbon cylinder. However, the points of discord here are whether the metal is in solid or liquid form, whether this diffusion is volume diffusion or surface diffusion, whether the actual catalyst for CNT growth is the pure metal or metal carbide, etc. Let us now review some important *in-situ* electron microscopic studies on these aspects.

5.1. Physical State of the Catalyst

The first effort to observe the carbon filament growth process *in-situ* was made by Baker et al.[8] By installing a gas-reaction cell in the TEM specimen chamber, they were able to perform carbon fiber growth in a temperature range of 600–1200 °C at different gas pressures up to 225 torr (maximum), while the TEM column was maintained at sufficiently low temperature and pressure suitable for electron microscopy. For acetylene decomposition on nickel catalyst supported on silica and graphite supports at 600 °C, they clearly observed that the metal particles changed it shape and moved up with a trail of carbon deposit (30–50 nm diameter). From the changing shape of the metal particle during fiber growth, they assumed that the catalyst was in liquid phase. The activation energy calculated for this growth was nearly same as the activation energy of carbon diffusion in liquid nickel; hence they suggested that carbon diffuses through the bulk metal and the fiber growth rate is diffusion-controlled. Similar tip-growth process was observed with Fe, Co and Cr catalysts.[9] But in the case of acetylene decomposition on bimetallic (Pt–Fe) catalyst, the catalyst was observed to remain static on the substrate, while the carbon filament went on growing up. This led them to enunciate base-growth model.[10] It was explained that strong interaction between Pt–Fe and SiO_2 substrate kept the metal particle anchored to the substrate surface, and carbon precipitation occurred from the free upper face of the particle. Temperature and concentration gradients were thought to be the main driving forces for the continued growth dynamics. The filament growth was seen to be ceased when the particle was fully covered with the carbon cloud, but it could be re-activated by exposure to either hydrogen or oxygen at higher temperatures.[8] Later, however, many scientists reported base-grown CNTs from Fe and Co catalysts on Si and SiO_2 substrates.[7, 60, 146, 147] This indicates that the same set of hydrocarbon, catalyst and substrate may act differently in slightly different experimental conditions (temperature, pressure, etc.).

In 1984 Gary Tibbetts explained why catalytically-grown carbon nanofibers were tubular.[148] Because the surface free energy of the (002) basal plane of graphite is exceptionally low, the free energy required for a filament growth is minimum when graphite is in the form of a seamless cylinder circumfering the metal. And the inner core is hollow because inner cylindrical planes of small diameter would be highly strained, energetically unfavorable to form. He also explained the CNT growth mechanism with a vapor–liquid–solid (VLS) model, originally formulated for Si, Ge whiskers and many other crystals.[149]

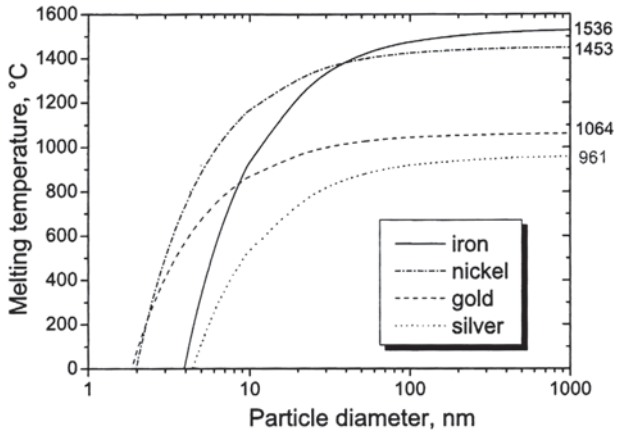

Fig. 4. Melting temperature of selected metals as a function of particle diameter. Reprinted with permission from [57], A. Moisala et al., *J. Phys.: Condens. Mater.* 15, S3011 **(2003)**. © 2003, IOP Publishing Ltd.

Although this model is convincing and acceptable to a great extent, it is often doubted how Fe, Co, Ni etc (normal melting point ~1500 °C) could be in liquid state within 600–900 °C, the growth temperature of typical CNTs in CVD. Here it is important to note that the melting point of nanoparticles below 10 nm falls abruptly (Fig. 4). For instance, a 5-nm Fe and Co particle can melt at about 850 °C and 640 °C, respectively. These values (melting points) fall on the border line casting the probability of 50–50 for both solid and liquid states of the metal. So it is still hard to say on the metal's physical state authoritatively. However, recalling that hydrocarbon decomposition on metal surface is an exothermic reaction, it is likely that the extra heat generated during hydrocarbon decomposition helps metal liquefaction to some extent. Hence the opinion of active catalyst being in liquid phase wins, as reported by many scientists for SWCNT growth.[150, 151] But then what about the case of MWCNTs which usually grow on bigger (>20 nm) metal particles? Bigger particles must be in solid phase; and in turn, MWCNT would involve a different growth mechanism than that of SWCNT!!

Another reasonable disagreement between the SWCNT and MWCNT growth is on the existence of temperature gradient inside the metal catalyst. Baker's explanation of temperature-gradient driven fiber growth might be applicable to MWCNTs which involve big catalyst particles. In the case of SWCNTs, however, it is very hard to imagine a significant temperature gradient within a particle of 1–2 nm. Hence SWCNT growth must be driven by the carbon concentration gradient during the process. Ding et al. have reported a molecular dynamics study of SWCNT growth without temperature gradient which supports this view.[152]

5.2. Mode of Carbon Diffusion

Another highly-debatable question is whether the so-called diffusion of carbon species through metal particle is surface diffusion or bulk (volumetric) diffusion. Endo's group who extensively carried out benzene decomposition on iron catalyst at 1100 °C,[12] argued that hollow fiber could form only by surface diffusion on the metal particle, as earlier proposed by Baird et al.[6, 7] In 2004, a Danish group, Helveg et al., succeeded in observing MWCNT growth from methane decomposition at 500 °C on Ni catalyst in a high-resolution TEM.[153] They noted that, throughout the growth process, the nickel cluster remained crystalline with well-faceted shapes (Fig. 5). The graphite layers were

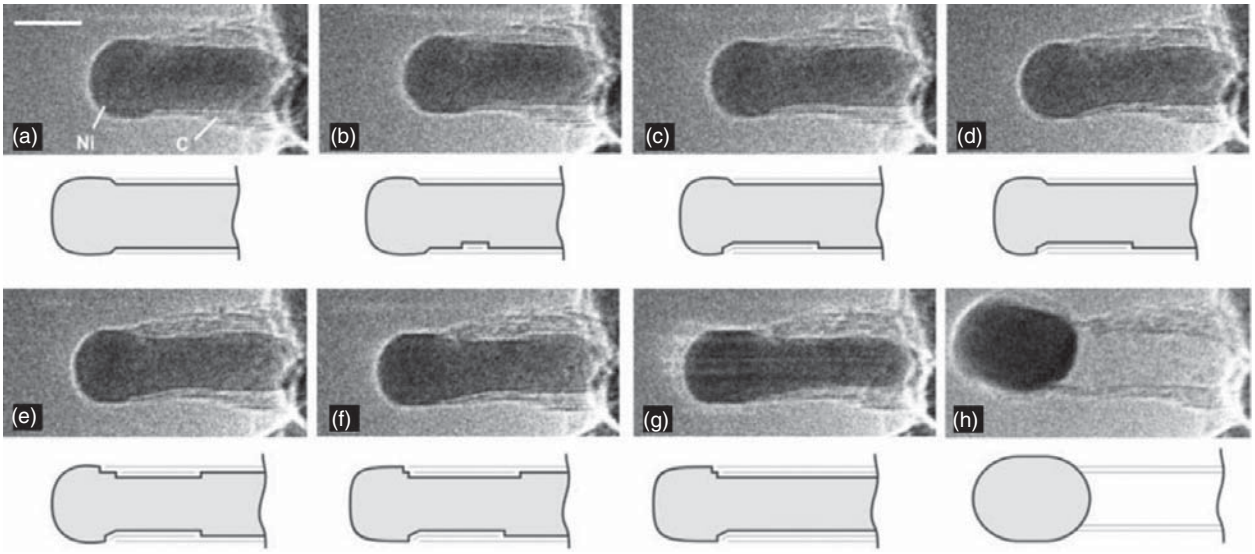

Fig. 5. *In situ* HRTEM image sequence of a growing carbon nanofiber. Images (a–h) illustrate one cycle in the elongation/contraction process. Drawings are included to guide the eye in locating the positions of mono-atomic Ni step-edges at the graphene–Ni interface. Scale bar = 5 nm. Reprinted with permission from [153], S. Helveg et al., *Nature* 427, 426 **(2004)**. © 2004, Nature Publishing Group.

found to grow as a consequence of dynamic interaction between carbon and nickel atoms. 'Surface atoms' of the nickel cluster moved up and down, in and out (continuously changing the metal's surface texture) as if they were knitting a graphene sheet out of the surrounding carbon atoms. The nanocluster shape was periodically changing its shape from spherical to cylindrical to align the graphene layers around them. The authors proposed that the monoatomic steps on the cluster boundary played a key role in anchoring carbon atoms and weaving the graphene network. This observation reveals that the catalyst cluster is in solid phase and the carbon diffusion is a surface diffusion around the catalyst.

Later, Raty et al. reported a molecular dynamics simulation study of the early stages of SWCNT growth on metal nanoparticles.[154] They showed that carbon atoms diffuse only on the outer surface of the metal cluster. At first, a graphene cap is formed which floats over the metal, while the border atoms of the cap remain anchored to the metal. Subsequently, more C atoms join the border atoms pushing the cap up and thus constituting a cylindrical wall (Fig. 6). In 2007, Robertson' group also reported similar findings by *in-situ* TEM observation of CNT growth.[155] These evidences also explain the general experience that small nanoparticles are crucial for SWCNT formation. Small metal clusters (1–2 nm) have steep sharp edges (atomic steps); hence they possess high catalytic activity and are capable to form high-strain SWCNTs. With the increasing cluster size the sharpness of the atomic steps at the boundary decreases and so does their catalytic activity. Therefore, bigger metal clusters (5–20 nm) form less-strained MWCNTs. Too big clusters (viz. 100 nm) acquire almost spherical boundary with no sharp steps; that is why they do not form CNTs at all.

Quite intriguingly, however, two months after Hoffmann's report,[155] Terrones and Banhart group reported an exciting observation of CNT formation in an HRTEM by simply holding a metal-encapsulated MWCNT at 600 °C under electron beam (300 kV) for 90 min.[156] Carbon atoms

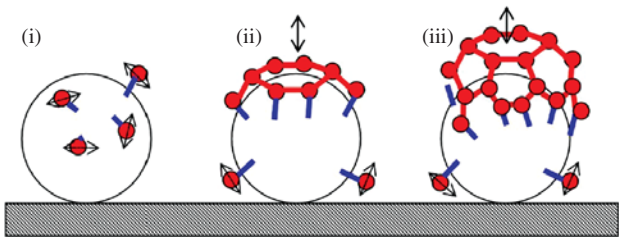

Fig. 6. Schematic representation of the basic steps of SWCNT growth on a Fe catalyst, as observed in *ab initio* simulations. (i) Diffusion of single C atoms (red spheres) on the surface of the catalyst. (ii) Formation of an sp^2 graphene sheet floating on the catalyst surface with edge atoms covalently bonded to the metal. (iii) Root incorporation of diffusing single C atoms (or dimers). Reprinted with permission from [154], J. Y. Raty et al., *Phys. Rev. Lett.* 95, 096103 **(2005)**. © 2005, American Physical Society.

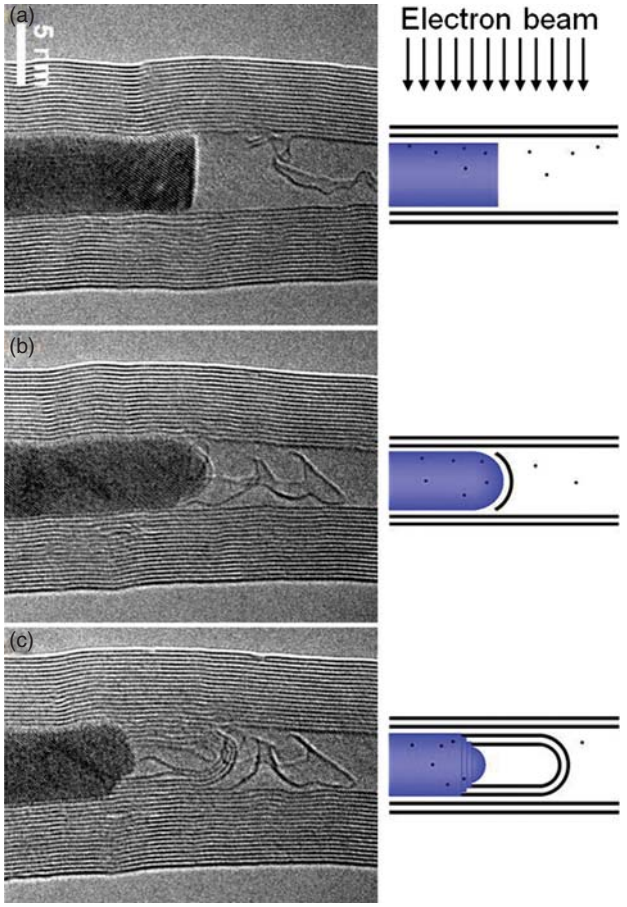

Fig. 7. *In-situ* observation of CNT growth under HRTEM. (a) Electron beam knocks some carbon atoms from the MWCNT side walls into the encapsulated metal cluster. (b) The metal cluster reshapes its flat cross section into a convex dome and a carbon cap appears over the dome. (c) At the base of the metal dome, atomic steps develop and new MWCNTs emerge coaxial to the original MWCNT. [Courtesy: M. Terrones]

from the side walls (the existing graphite layers around the encapsulated metal) got injected into the metal bulk and emerged in the form of new SW, DW and MWCNTs of smaller diameters coaxial to the original MWCNT (Fig. 7). Such a prolonged observation of the CNT-growth dynamics (atom-by-atom) clearly evidences bulk diffusion. Nevertheless, we should note that this observation was an exclusive case of rearrangement of the carbon-iron ensemble inside a constrained nanoreactor (the original MWCNT) under high-energy electron-beam irradiation, a situation far away from usual CVD conditions. Hence such bulk diffusion cannot be conceptualized as a general CNT growth mechanism.

In the context of the changing metal shape during CVD, it is pertinent to mention another aspect of the CNT growth. Many a time we encounter CNTs with their graphene layers inclined to the tube axis (herringbone or stacked-cup structure). It is puzzling to think how they form. Keeping in mind that graphite layers grow preferentially on selected crystal planes of metal, this can be

understood as follows. The shape of the catalyst metal cluster acts as a template for the surrounding graphene layers. Nanoclusters (say, 10–20 nm Ø) under suitable thermodynamic conditions tend to form an elongated cylindrical shape (viz., 3 nm Ø) so that CNTs grow with the graphene layers parallel to the tube axis. Under certain (different) thermodynamic conditions the metal clusters tend to become pear-shaped, giving birth to graphene layers parallel to their inclined facets. This usually happens with bigger clusters (say, 100 nm) or for alloy catalysts.[157] When it comes to explain how such open-edged nanographenes are energetically stable, scientists suggest that those dangling bonds at the edges of the stacked graphite platelets are stabilized with the hydrogen atoms expelled from the hydrocarbon (or from the H_2 supply).[158] Such a fiber is known as graphite whisker, and many people do not consider that as a CNT.

5.3. Chemical State of the Catalyst

Another frequently debated point in the CNT growth mechanism is about the chemical state of the active catalyst. Most common concept is that the starting catalyst material (pre-deposited on substrates) is usually in oxide form. Even if we deposit fresh metal nanoparticles on a substrate, the nanoparticles are quickly oxidized when exposed to oxygen during the substrate transfer to the CVD reactor. During CVD, hydrogen gas is supplied to reduce the metal oxide into pure metal upon which hydrocarbon decomposition and subsequent diffusion leads to the CNT growth. Even when no hydrogen is supplied externally, the hydrogen atoms liberated from the hydrocarbon decomposition on the catalyst surface are likely to serve the same. However, there are many conflicting reports right from the early-stage CVD experiments. Baker and many others proposed that pure metal is the active catalyst,[159, 160] while Endo and many others detected the encapsulated particles (in the CNTs) to be iron carbide.[12, 161, 162]

Among recent reports, Yoshida et al. performed atomic-scale *in-situ* observation of acetylene decomposition on Fe catalyst at 600 °C and 10^{-2} torr.[163] Both SWCNT and MWCNT were clearly observed to be growing from metal particles rooted on the substrate as in base-growth model; however, the metal's shape was slightly fluctuating. Electron diffraction analysis of the metal clusters in each frame was reported to match with that of iron carbide in cementite (Fe_3C) form. Accordingly, the authors concluded that the active catalyst was in fluctuating solid state of iron carbide; the carbon diffusion was volumetric; and all layers of the MWCNTs grew up simultaneously, at the same growth rate. However, latest *in-situ* electron microscopy and XPS analysis by Wirth et al. emphatically advocate that the catalyst exists in pure metallic form: right from the CNT nucleation to the growth termination.[164] When the CNT growth ceases due to catalyst poisoning with excess carbon, that supersaturated metal–carbon ensemble crystallizes in carbide form upon cooling.[162] Confusion persists because the lattice constants of iron and iron carbide are very close; and for nanoparticles, some distortion in the lattice constants is likely due to the small-size effect. These diversities of observation unambiguously reflect that we have not matured enough to understand the world inside the nanotubes. Hence the research must go on in search of the fact.

6. MASS PRODUCTION OF CNTs

6.1. Mass Production of CNTs from Conventional Precursors

Since CVD is a well-known and established-industrial process, CNT production by CVD is easy to scale up. Several research groups translated their laboratory methods to large scale. Smalley's group developed the high pressure carbon monoxide decomposition technique (known as HiPco) for mass production of SWCNTs.[29] In this technique, iron pentacarbonyl catalyst liberates iron particles *in-situ* at high temperature, whereas the high-pressure (~10 atmosphere) of carbon monoxide enhances the carbon feedstock many folds, which significantly speeds up the disproportionation of CO molecules into C atoms and thus accelerates the SWCNT growth. Reported yield of HiPco process is ~0.45 g/h.[165] The product is commercially available at Carbon Nanotechnologies Inc. (USA), which is reported to have a production capacity of 65 g/h.[166] Dai's group has also scaled up SWCNT production from methane pyrolysis over Fe–Mo bimetallic catalyst supported on sol–gel derived alumina-silica multicomponent material. Their process yields ~1.5 g SWCNTs over 0.5 g catalyst hybrid as a result of 30 min CVD.[167] Maruyama's alcohol CVD technique[45] is also adopted by Toray Industries Inc. (Japan) with a reported capacity of 15 g/h; while Hata's technique[53] at AIST (Japan) can produce ~100 g/h.[166]

As for MWCNTs, Endo's group developed his method of benzene pyrolysis on iron catalyst[15] into a continuous process for mass production. In his process metal catalyst, benzene, and Ar/H_2 gases are fed from the upper end of a vertical furnace, and the resulting CNTs are collected from the lower end. CNT growth occurs while the catalyst particles are falling down (floating) through the furnace at 1100 °C.[168] The product is commercialized by Showa Denko KK (Japan) which is reported to have a production capacity of 16 kg/h.[166] Nagy's technique of acetylene CVD on various porous materials was also brought up to industrial level by Nanocyl (Belgium) producing ~1 kg/h MWCNTs.[67, 69] Fei's group developed a nano-agglomerate fluidized-bed reactor (1 m long and 25 cm Ø quartz cylinder) in which continuous decomposition of ethylene gas on Fe–Mo/vermiculite catalyst at 650 °C can yield up to 3 kg/h aligned MWCNT bundles.[169] Apart

from these university-venture-business associates, many other companies are also there in CNT business. To name some, Hyperion Catalysis International, Inc. USA (8 kg/h), Nano Carbon Technologies Co. Ltd. Japan (5 kg/h), Sun Nanotech Co. Ltd. China (0.6 kg/h), Shenzhen Nano-Technologies Port Co. Ltd. China (5 kg/h).[166]

As per WTEC survey report,[166] the consolidated CNT production capacity of the world today is ∼300 tons MWCNTs and ∼7 tons SWCNTs per year, while their expected demand would exceed 1000 tons/year in the near future. The present price of commercially available MWCNTs is ∼$1/g, while that of SWCNTs is ∼$100/g. At this rate, CNT-based products would be about 10 times costlier than prevalent products. Hence the scientists and engineers have a great responsibility to develop more cost-effective production techniques to bring down the prices to $100/kg and $10,000/kg for MWCNTs and SWCNTs respectively.

A good sign is that CVD-based CNT technique is progressing fast, and innumerous companies are emerging. However, a common problem of mass-produced CNTs is that their purity decreases with the increasing yield. CNT properties are easy to control in small reactors, as used in academic laboratories. When the same technique is transferred to big reactors, purity goes down and diameter distribution broadens drastically. This problem warrants that we must find more simple, more refined technique which could be translated to large scale with the same control. Moreover, in view of the growing environmental concern and increasing CNT demand, efforts should be made to develop a sustainable technology. Rapidly diminishing fossil fuel, alarms that methane-, acetylene-, benzene-based CNT technology would not be sustainable. Hence we must explore regenerative, renewable materials for mass production of CNTs.

6.2. Mass Production of CNTs from Camphor

Researchers at Meijo University have reported *gigas growth* of CNTs from camphor.[119] In a simple CVD reactor (1 m long and 55 mm Ø quartz tube in a horizontal split furnace), 30-min-CVD of 12 g camphor over 0.6 g Fe–Co-impregnated zeolite powder at 650 °C yields 6.6 g CNTs with an as-grown purity of >91% (Fig. 8). The volume of the zeolite bed before CVD is 1.5 mm, which inflates

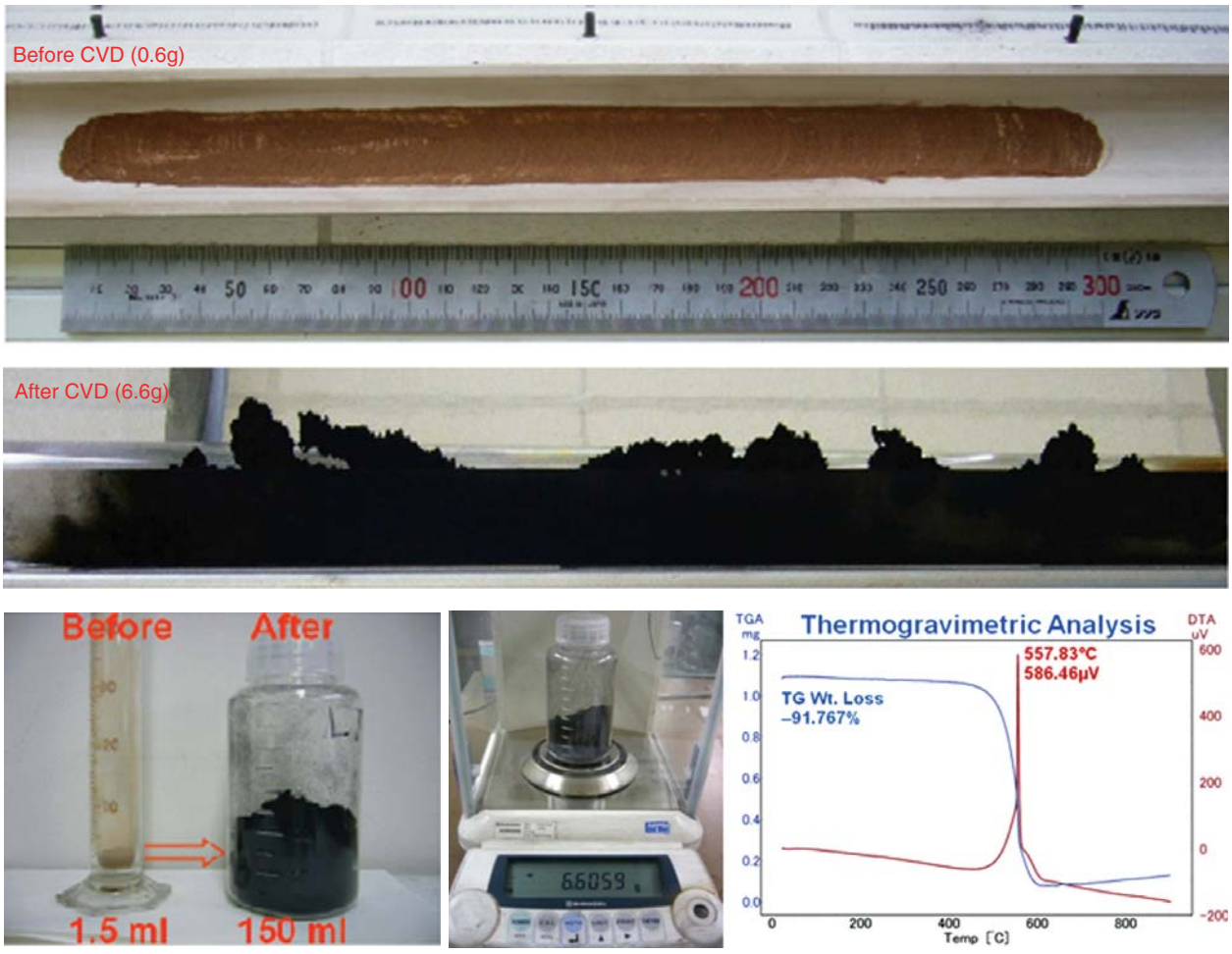

Fig. 8. Photographs of the zeolite bed before and after CVD; and TG analysis of as-grown CNTs.

to 150 mm owing to a gigantic CNT growth (10,000%). Hence the authors call it *gigas growth*. In this process, camphor-to-CNT production efficiency is >50%, which is much higher than that reported from any CNT precursor in an academic laboratory set-up. Here it is to be noted that the carbon content of camphor is approximately 79 wt%. So, with respect to the carbon content in the feed stock, net carbon-to-CNT conversion efficiency comes out to be 61 wt%. There are plenty of reports of large-scale CNT synthesis; but most of them express the yield either on the basis of TEM observation, or wait gain relative to the catalyst. From industrial point of view, the product yield must be quoted with respect to the raw material used. CNT literature largely lacks this figure of merit. To compare camphor's efficiency with that of other precursors, CVDs of a few liquid precursors were carried out on the same set up, in the same conditions. CVD of 12 g ethanol and benzene yielded about 2 g and 3 g CNTs, respectively; much lower than the camphor case (6 g). Here it is arguable that every precursor has its own set of best conditions. Ethanol or benzene cannot give their best yields at the condition optimized for camphor. So, more systemic study is required to compare different precursors. Recently, Montoro et al. carried out a comparative study of several alcohols and ketones as a CNT precursor over Mn–Co-impregnated zeolite support at 600 °C.[170] Acetone was found the best precursor (better that ethanol). This report is in agreement with our experience that camphor (a member of ketone family) stood the best. More recently, Musso et al. also investigated thermal decompositions of camphor, cyclohexanol and ethanol at 900 °C using ferrocene catalyst; and found that camphor gave the highest CNT yield with best crystallinity.[171] On the other hand, Das et al. studied the effect of feedstock and process conditions on CNT synthesis from several aromatic hydrocarbons (unfortunately, camphor was not there).[172] They systematically calculated the CNT yield with respect to the feedstock, and found that carbon-to-CNT conversion efficiency ranged within 20–39%. On that scale, camphor scores very high (61%).

The high CNT-production efficiency of camphor ($C_{10}H_{16}O$) may be attributed to several factors.

(i) Cage-like carbon structure offers ease of transformation into fullerene and CNTs.

(ii) Ring-based CNT-growth process is supposed to lead to higher growth rate.

(iii) Carbon-rich precursors have shown higher CNT yields.

(iv) Abundance of hydrogen and presence of oxygen in camphor may have a good coordination in reducing metal oxide and etching amorphous carbon.

However, more-elaborated experiments and theoretical supports are required to establish these reasons. Enthusiastic researchers are encouraged to take up these challenges.

6.3. Camphor versus Conventional CNT Precursors

As compared to conventional CNT precursors such as CH_4, C_2H_4, C_2H_2, C_6H_6, camphor ($C_{10}H_{16}O$) is carbon-rich, hydrogen-rich, and oxygen-present. It is thought that the bi-cyclic cage-structure of camphor plays a vital role in such an efficient CNT growth. Most probably, the hexagonal and pentagonal carbon rings of camphor construct CNTs as a basic building block: without breaking into atomic carbon. Researchers often use to mix a small amount of hydrogen gas in the carrier gas to reduce metal oxide into pure metal catalyst. Abundance of hydrogen in camphor serves this purpose to a great extent and eliminates the need of additional hydrogen mixing in the carrier gas. Moreover, the oxygen atom present in camphor molecule helps oxidizing amorphous carbon *in-situ*, as proposed by Maruyama et al.[45] Thus every atom of camphor has a positive role towards CNT synthesis. A probable growth mechanism of CNTs from camphor was first reported in 2003.[117] Later, a Chinese group carried out *in-situ* mass spectroscopy of benzene CVD and supported the ring-based CNT growth hypothesis.[173] In particular, low-temperature camphor CVD (650 °C) rules out the possibility of spontaneous (uncatalyzed) decomposition of camphor vapor in the reactor, and results in CNTs free from amorphous carbon. There is no trace of carbon deposit in any portion of the quartz tube except on the zeolite bed.

6.4. Environment-Friendliness of Camphor CVD

The United States Environmental Protection Agency has formulated *12 Principles of Green Chemistry* that explain what *green chemistry* means in actual practice.[174] Waste prevention, atom economy, energy efficiency and renewable feed stock are most vital points for an industrial process to be environmentally benign. Using those principles as a protocol, we can evaluate how environment-friendly this technique is. It is straightforward that the higher is the yield the lesser is the waste. Exhibiting highest CNT-production efficiency, camphor complies with the waste-prevention rule significantly. Moreover, as explained above, every atom of camphor plays a positive role in CNT synthesis, which accounts for maximum carbon-to-CNT conversion efficiency. This is a good example of atom economy. Further, by virtue of a low-temperature and atmospheric-pressure CVD process, the energy requirement of this technique is very low (as compared to high-temperature low-pressure CVD-CNT processes). Hence certainly it is an energy-efficient method. And last but not the least, the main raw material—camphor—being an agricultural product, is absolutely a regenerative feedstock; so there is no danger of depleting a natural resource. Thus, camphor-based CNT synthesis technique complies with the principles of *green chemistry* to a great extent. This work has attracted the attention of industrial ecologists.[175]

6.5. Industrial Production of CNTs from Camphor

Camphor CVD has been successfully scaled up to industrial production of MWCNTs at Meijo Nano Carbon Co. Ltd., Japan. A big quartz tube (2 m long and 0.25 m Ø) installed in an especially-designed rotary kiln (Takasago Co. Ltd., Japan) is used as a CVD reactor. Camphor and catalyst-loaded zeolite powder are simultaneously fed in the reactor from the left and right ends, respectively, through two speed-controllable feeders. The quartz tube is slightly inclined and keeps on rotating about its axis, so that the zeolite powder falling on the right end of hot zone slides down the slope; and by the time it reaches the left end of the hot zone, CNTs would have efficiently grown onto it. As-grown CNTs safely fall down into a reservoir at the left end. The system can run continuously for hours. Aaverage production rate is about 1 kg/h and the purity of as-grown MWCNTs is about 90%. Due to extremely low price of camphor ($10/kg), the expected production cost of as-grown CNTs is very low ($100/kg).

REVIEW

7. EXISTING CHALLENGES AND FUTURE DIRECTIONS

In the foregoing sections, we raised several questions on the role of precursor, catalyst, catalyst support, growth mechanism and mass production, and indicated possible directions. In addition to those basic issues, other growth-related challenges are briefly outlined below.

1. Researchers have succeeded in minimizing the diameter distribution of SWCNTs up to some extent.[176] However, synthesis of SWCNTs of a given diameter is yet to be achieved.[177] It would be possible only when we have the catalyst particles all of exactly the same diameter (say, 0.5 nm).
2. Chirality control is even more challenging. Re-growth from ordered arrays of open-ended SWCNTs may help up to some extent.[178] Alternatively, we have to develop proper separation methods that could first sort out CNTs according to metallic or semiconducting tubes and then select tubes of certain chirality.
3. In MWCNTs, control on the number of walls is another big challenge. Synthesis of thin MWCNTs (3–6 walls) is a better choice than thick MWCNTs.[179, 180]
4. Growth of isolated CNTs has not yet reached a mature stage. There are indications that even a single CNT does not possess the same diameter and chirality over the entire length. How can we solve it?
5. Researchers have succeeded in growing CNTs from almost all metals.[181] However, we do not know how different metals affect physical, chemical, electronic and optical and magnetic properties of as-grown CNTs. If we could discover any correlation between the type of the metal used and the property of the CNT grown, we would be able to grow CNTs of selective properties.
6. What is/are the determining steps in CNT nucleation and growth? Having known these steps, the CNT growth rate could be increased for mass production.[182]
7. The exact role of H_2, O_2 and H_2O in CNT growth is yet to be clarified.[183] Simultaneous presence of reducing as well as oxidizing agents in the reaction zone makes it ambiguous whether amorphous carbon is etched by atomic hydrogen, oxygen or water. Are they really essential?[54]
8. Researchers have succeeded in bringing down the CNT growth temperature to ~400 °C in low-pressure CVD.[184] However, low-pressure CVD greatly reduces the growth rate and yield. Low-temperature CNT growth must be devised at atmospheric pressure for high yields of CNTs.
9. Many technological applications are looking for room-temperature CNT growth which is still a dream, so far as thermal CVD is concerned.
10. Mass-produced CNTs usually contain catalyst particles or support materials as impurity. Post-deposition purification greatly reduces the CNT quality and final output. More thoughts should be given to achieve high-purity in as-grown state.
11. CVD-grown CNTs (especially low-temperature MWCNTs) have poor crystallinity. With a suitable combination of different catalysts, it should be possible to get better-crystallinity CNTs.
12. Recent metal-free oxygen-assisted CNT growth is a breakthrough.[99–101] It must be scaled up to mass production of high-purity CNTs.
13. Carbon–metal phase diagram needs to be reconstructed, especially for 1–5 nm range relevant to CNT growth.[185]
14. All extraordinary properties of CNTs are predicted for atomically-perfect CNTs. To make those predictions true, it is of prime importance to develop new techniques to monitor and remove defects *in-situ*.
15. Lack of quality control and assessment of CNTs synthesized by different groups by different methods does not allow us to get correct product details. Analytical sampling of CNTs obtained from different sources at an authorized standard laboratory would reveal exact merits and demerits of different techniques, which would in turn help us explore combinations of techniques toward higher-yield, higher-purity and lower-cost mass production.

What we have mentioned above are only growth-related challenges. There are many application-related challenges whose mention is beyond the scope of this review.

8. CONCLUDING REMARKS

In 2000 Rick Smalley said about CNTs, "Buckytubes are in high school now." After 10 years of his statement, we feel that CNTs are now in university; they have not yet graduated and joined their jobs out. As we have seen in the foregoing sections, despite great progresses over the years, there are many basic issues concerning the CNT

growth mechanism which are still not clear. Contradictory observations of CNT growth under electron microscopy by different groups suggest that the mechanism is extremely sensitive to each parameter such as carbon precursor, metal catalyst, particle size, temperature, pressure. Even a minor change in any of these parameters leads the growth in critically different directions. Catalysis is the main stem of CVD-CNT technique; and it seems that we have not yet utilised the best of catalysis in this field. *Nano*-catalyst materials are needed to be developed and investigated in more detail. In principle, with the use of a suitable catalyst, the CVD temperature can be brought down to room temperature. By identifying the growth-limiting steps it should be possible to control the diameter and chirality of the resulting CNTs. To comply with the environmental concerns, renewable materials should be explored as CNT precursors. In view of the expected giant demand of CNTs in the near future, industrial production of CNTs should be carried out with far-sighted thoughts for long-term sustainability. Fossil-fuel based CNT-production technology would not be sustainable. The unanswered questions about growth mechanism and the existing challenges concerning the growth control will keep the CNT researchers engaged for a long time. In quest for knowledge, in pursuit of perfection, and for contributing to science and society, the CNT research must go on.

Acknowledgments: This work was financially supported by the Japan Society for the Promotion of Science (Grants-in-aid for Scientific Research), the Ministry of Economy Trade and Industry (Regional Resources R&D), and the Ministry of Education, Culture, Sports, Science and Technology (Regional Innovation Creation R&D). The authors are grateful to Dr. Toshio Kurauchi (Former Vice President, Toyota Central R&D Labs Inc.), Mr. Takeshi Hashimoto (President, Meijo Nano Carbon Co. Ltd.), Mr. Akira Kagohashi (Managing Director, Takasago Industry Co. Ltd.) and Mr. Hirotaka Masuoka (Director, Masuoka Ceramic Materials Co. Ltd.), whose joint efforts drove our work from laboratory to industry. Mukul Kumar thanks Dr. Debabrata Pradhan for his great help on the references.

References and Notes

1. L. V. Radushkevich and V. M. Lukyanovich, *Zh. Fizich. Khim.* (in Russian) 26, 88 **(1952)**.
2. P. A. Tesner and A. I. Echeistova, *Doklady Akad. Nauk USSR* 87, 1029 **(1952)**.
3. W. R. Davis, R. J. Slawson, and G. R. Rigby, *Nature* 171, 756 **(1953)**.
4. L. J. E. Hofer, E. Sterling, and J. T. McCartney, *J. Phys. Chem.* 59, 1153 **(1955)**.
5. P. L. Walker, J. F. Rakszawski, and G. R. Imperial, *J. Phys. Chem.* 63, 133 **(1959)**.
6. T. Baird, J. R. Fryer, and B. Grant, *Nature* 233, 329 **(1971)**.
7. T. Baird, J. R. Fryer, and B. Grant, *Carbon* 12, 591 **(1974)**.
8. R. T. K. Baker, M. A. Barber, P. S. Harris, F. S. Feates, and R. J. Waite, *J. Catalysis* 26, 51 **(1972)**.
9. R. T. K. Baker, P. S. Harris, R. B. Thomas, and R. J. Waite, *J. Catalysis* 30, 86 **(1973)**.
10. R.T. K. Baker and R. J. Waite, *J. Catalysis* 37, 101 **(1975)**.
11. T. Koyama, M. Endo, and Y. Onuma, *Jpn. J. Appl. Phys.* 11, 445 **(1972)**.
12. A. Oberlin, M. Endo, and T. Koyama, *J. Cryst. Growth* 32, 335 **(1976)**.
13. R. T. K. Baker and P. S. Harris, Chemistry and Physics of Carbon, edited by P. L. Walker and P. A. Thrower, Marcel Dekker, NY **(1978)**, Vol. 14, p. 83.
14. R. T. K. Baker, *Carbon* 27, 315 **(1989)**.
15. M. Endo, *Chemtech* 18, 568 **(1988)**.
16. M. S. Dresselhaus, G. Dresselhaus, K. Sugihara, I. L. Spain, and H. A. Goldberg, Graphite Fibers and Filaments, Springer-Verlag, Berlin **(1988)**.
17. J. S. Speck, M. Endo, and M. S. Dresselhaus, *J. Cryst. Growth* 94, 834 **(1989)**.
18. S. Iijima, *Nature* 354, 56 **(1991)**.
19. P. Schultzenberger and L. Schultzenberger, *C.R. Acad. Sci. Paris* 111, 774 **(1890)**.
20. M. Endo, K. Takeuchi, K. Kobori, K. Takahashi, H. W. Kroto, and A. Sarkar, *Carbon* 33, 873 **(1995)**.
21. S. B. Sinnott, R. Andrews, D. Qian, A. M. Rao, Z. Mao, E. C. Dickey, and F. Derbyshire, *Chem. Phys. Lett.* 315, 25 **(1999)**.
22. K. Hernadi, A. Fonseca, J. B. Nagy, D. Bernaerts, and A. A. Lucas, *Carbon* 34, 1249 **(1996)**.
23. J. Kong, A. M. Cassell, and H. Dai, *Chem. Phys. Lett.* 292, 567 **(1998)**.
24. S. Fan, M. Chapline, N. Frankline, T. Tombler, A. M. Cassel, and H. Dai, *Science* 283, 512 **(1999)**.
25. B. C. Satiskumar, A. Govindaraj, and C. N. R. Rao, *Chem. Phys. Lett.* 307, 158 **(1999)**.
26. W. Z. Li, S. Xie, L. X. Qian, B. H. Chang, B. S. Zou, W. Y. Zhou, R. A. Zhao, and G. Wang, *Science* 274, 1701 **(1996)**.
27. R. Sen, A. Govindaraj, and C. N. R. Rao, *Chem. Phys. Lett.* 267, 276 **(1997)**.
28. B. Q. Wei, R. Vajtai, Y. Jung, J. Ward, R. Zhang, G. Ramanath, and P. M. Ajayan, *Nature* 416, 495 **(2002)**.
29. P. Nikolaev, M. J. Bronikowski, R. K. Bradley, F. Rohmund, D. T. Colbert, K. A. Smith, and R. E. Smalley, *Chem. Phys. Lett.* 313, 91 **(1999)**.
30. M. Endo, H. Fijiwara, and E. Fukunaga, *18th Meeting Japanese Carbon Society*, Japanese Carbon Society, Saitama, December **(1991)**, p. 34.
31. M. Endo, K. Takeuchi, S. Igarashi, K. Kobori, M. Shiraishi, and H. W. Kroto, *19th Meeting Japanese Carbon Society*, Japanese Carbon Society, Kyoto, December **(1992)**, p. 192.
32. M. Endo, K. Takeuchi, S. Igarashi, K. Kobori, M. Shiraishi, and H. W. Kroto, *J. Phys. Chem. Solids* 54, 1841 **(1993)**.
33. M. Jose-Yacaman, M. Miki-Yoshida, L. Rendon, and J. G. Santiesteban, *Appl. Phys. Lett.* 62, 657 **(1993)**.
34. Z. Liua, R. Cheb, Z. Xu, and L. Peng, *Synth. Met.* 128, 191 **(2002)**.
35. N. Li, X. Chen, L. Stoica, W. Xia, J. Qian, J. Abmann, W. Schuhmann, and M. Muhler, *Adv. Mater.* 19, 2957 **(2007)**.
36. O. A. Nerushev, S. Dittmar, R. E. Morjan, F. Rohmund, and E. E. B. Campbell, *J. Appl. Phys.* 93, 4185 **(2003)**.
37. R. E. Morjan, O. A. Nerushev, M. Sveningsson, F. Rohmund, L. K. L. Falk, and E. E. B. Campbell, *Appl. Phys. A* 78, 253 **(2004)**.
38. H. Dai, A. G. Rinzler, P. Nikolaev, A. Thess, D. T. Colbert, and R. E. Smalley, *Chem. Phys. Lett.* 260, 471 **(1996)**.
39. H. M. Cheng, F. Li, X. Sun, S. D. M. Brown, M. A. Pimenta, A. Marucci, G. Dresselhaus, and M. S. Dresselhaus, *Chem. Phys. Lett.* 289, 602 **(1998)**.
40. B. C. Satishkumar, A. Govindaraj, R. Sen, and C. N. R. Rao, *Chem. Phys. Lett.* 293, 47 **(1998)**.

REVIEW

41. J. H. Hafner, M. J. Bronikowski, B. R. Azamian, P. Nikolaev, A. G. Rinzler, D. T. Colbert, K. A. Smith, and R. E. Smalley, *Chem. Phys. Lett.* 296, 195 **(1998)**.

42. E. Flahaut, A. Govindaraj, A. Peigney, C. Laurent, and C. N. R. Rao, *Chem. Phys. Lett.* 300, 236 **(1999)**.

43. A. Gruneis, M. H. Rummeli, C. Kramberger, D. Grimm, T. Gemming, A. Barreiro, P. Ayala, T. Pichler, H. Kuzmany, C. Schamann, R. Pfeiffer, J. Schumann, and B. Büchner, *Physica Status Solidi B* 243, 3054 **(2006)**.

44. S. Maruyama, Y. Miyauchi, T. Edamura, Y. Igarashi, S. Chiashi, and Y. Murakami, *Chem. Phys. Lett.* 375, 553 **(2003)**.

45. S. Maruyama, R. Kojima, Y. Miyauchi, S. Chiashi, and M. Kohno, *Chem. Phys. Lett.* 360, 229 **(2002)**.

46. S. Okubo, T. Sekine, S. Suzuki, Y. Achiba, K. Tsukagoshi, Y. Aoyagi, and H. Kataura, *Jpn. J. Appl. Phys.* 43, L396 **(2004)**.

47. A. Gruneis, M. H. Rummeli, C. Kramberger, A. Barreiro, T. Pichler, R. Pfeiffer, H. Kuzmany, T. Gemming, and B. Buchner, *Carbon* 44, 3177 **(2006)**.

48. A. G. Nasibulin, A. Moisala, H. Jiang, and E. I. Kauppinen, *J. Nanopart. Res.* 8, 465 **(2006)**.

49. Y. Murakami, Y. Miyauchi, S. Chiashi, and S. Maruyama, *Chem. Phys. Lett.* 377, 49 **(2003)**.

50. Y. Murakami, S. Chiashi, Y. Miyauchi, M. Hu, M. Ogura, T. Okubo, and S. Maruyama, *Chem. Phys. Lett.* 385, 298 **(2004)**.

51. S. Maruyama, E. Einarsson, Y. Murakami, and T. Edamura, *Chem. Phys. Lett.* 403, 320 **(2005)**.

52. R. Xiang, E. Einarsson, J. Okawa, Y. Miyauchi, and S. Maruyama, *J. Phys. Chem. C* 113, 7511 **(2009)**.

53. K. Hata, D. N. Futaba, K. Mizuno, T. Namai, M. Yumura, and S. Iijima, *Science* 306, 1362 **(2004)**.

54. G. Zhong, S. Hofmann, F. Yan, H. Telg, J. H. Warner, D. Eder, C. Thomsen, W. I. Milne, and J. Robertson, *J. Phys. Chem. C* 113, 17321 **(2009)**.

55. F. Ding, P. Larsson, J. A. Larsson, R. Ahuja, H. Duan, A. Rosen, and K. Bolton, *Nano Lett.* 8, 463 **(2008)**.

56. H. Ago, T. Komatsu, S. Ohshima, Y. Kuriki, and M. Yumura, *Appl. Phys. Lett.* 77, 79 **(2000)**.

57. A. Moisala, A. G. Nasibulin, and E. I. Kauppinen, *J. Phys. Condens. Mater.* 15, S3011 **(2003)**.

58. R. Andrews, D. Jacques, A. M. Rao, F. Derbyshire, D. Qian, X. Fan, E. C. Dickey, and J. Chen, *Chem. Phys. Lett.* 303, 467 **(1999)**.

59. M. Kumar and Y. Ando, *Chem. Phys. Lett.* 374, 521 **(2003)**.

60. M. Kumar, K. Kakamu, T. Okazaki, and Y. Ando, *Chem. Phys. Lett.* 385, 161 **(2004)**.

61. D. Ding, J. Wang, Z. Cao, and J. Dai, *Carbon* 41, 579 **(2003)**.

62. T. Murakami, T. Sako, H. Harima, K. Kisoda, K. Mitikami, and T. Isshiki, *Thin Solid Films* 464, 319 **(2004)**.

63. B. Kitiyanan, W. E. Alvarez, J. H. Harwell, and D. E. Resasco, *Chem. Phys. Lett.* 317, 497 **(2000)**.

64. C. Mattevi, C. T. Wirth, S. Hofmann, R Blume, M. Cantoro, C. Ducati, C. Cepek, A. Knop-Gericke, S. Milne, C. Castellarin-Cudia, S. Dolafi, A. Goldoni, R. Schloegl, and J. Robertson, *J. Phys. Chem. C* 112, 12207 **(2008)**.

65. C. L. Cheung, A. Kurtz, H. Park, and C. M. Lieber, *J. Phys. Chem. B* 106, 2429 **(2002)**.

66. H. Hongo, M. Yudasaka, T. Ichihashi, F. Nihey, and S. Iijima, *Chem. Phys. Lett.* 361, 349 **(2002)**.

67. I. Willems, Z. Konya, J. F. Colomer, G. V. Tendeloo, N. Nagaraju, A. Fonseca, and J. B. Nagy, *Chem. Phys. Lett.* 317, 71 **(2000)**.

68. M. Kumar and Y. Ando, *Carbon* 43, 533 **(2005)**.

69. E. Couteau, K. Hernadi, J. W. Seo, L. T. Nga, C. Miko, R. Gaal, and L. Forro, *Chem. Phys. Lett.* 378, 9 **(2003)**.

70. J. F. Colomer, C. Stephan, S. Lefrant, G. Van-Tendeloo, I. Willems, Z. Konya, A. Fonseca, C. Laurent, and J. B. Nagy, *Chem. Phys. Lett.* 317, 83 **(2000)**.

71. J. Ward, B. Q. Wei, and P. M. Ajayan, *Chem. Phys. Lett.* 376, 717 **(2003)**.

72. H. Ago, K. Nakamura, S. Imamura, and M. Tsuji, *Chem. Phys. Lett.* 391, 308 **(2004)**.

73. K. Hernadi, A. Fonseca, J. B. Nagy, D. Bernaerts, A. Fudala, and A. A. Lucas, *Zeolites* 17, 416 **(1996)**.

74. N. Nagaraju, A. Fonseca, Z. Konya, and J. B. Nagy, *J. Mol. Catal. A* 181, 57 **(2002)**.

75. H. Ago, K. Nakamura, N. Uehara, and M. Tsuji, *J. Phys. Chem. B* 108, 18908 **(2004)**.

76. C. L. Pint, S. T. Pheasant, M. Pasquali, K. E. Coulter, H. K. Schmidt, and R. H. Hauge, *Nano Lett.* 8, 1879 **(2008)**.

77. S. Noda, K. Hasegawa, H. Sugime, K. Kakehi, Z. Zhang, S. Maruyama, and Y. Yamaguchi, *Jpn. J. Appl. Phys.* 46, L399 **(2007)**.

78. D. Yuan, L. Ding, H. Chu, Y. Feng, T. P. McNicholas, and J. Liu, *Nano Lett.* 8, 2576 **(2008)**.

79. D. Takagi, Y. Homma, H. Hibino, S. Suzuki, and Y. Kobayashi, *Nano Lett.* 6, 2642 **(2006)**.

80. S. Bhaviripudi, E. Mile, S. A. Steiner, A. T. Zare, M. S. Dresselhaus, A. M. Belcher, and J. Kong, *J. Am. Chem. Soc.* 129, 1516 **(2007)**.

81. D. Takagi, Y. Kobayashi, H. Hibino, S. Suzuki, and Y. Homma, *Nano Lett.* 8, 832 **(2008)**.

82. R. L. Vander Wal, T. M. Ticich, and V. E. Curtis, *Carbon* 39, 2277 **(2001)**.

83. W. Deng, X. Xu, and W. A. Goddard, *Nano Lett.* 4, 2331 **(2004)**.

84. X. Tao, X. Zhang, J. Cheng, Y. Wang, F. Liu, and Z. Luo, *Chem. Phys. Lett.* 409, 89 **(2005)**.

85. C. P. Deck and K. Vecchio, *Carbon* 44, 267 **(2006)**.

86. W. Zhou, Z. Han, J. Wang, Y. Zhang, Z. Jin, X. Sun, Y. Zhang, C. Yan, and Y. Li, *Nano Lett.* 6, 2987 **(2006)**.

87. X. Sun, Y. Zhang, R. Si, and C. Yan, *Small* 1, 1081 **(2005)**.

88. M. Ritschel, A. Leonhardt, D. Elefant, S. Oswald, and B. Buchner, *J. Phy. Chem. C* 111, 8414 **(2007)**.

89. D. Takagi, Y. Kobayashi, and Y. Homma, *J. Am. Chem. Soc.* 131, 6922 **(2009)**.

90. M. H. Rummeli, E. Borowiak-Palen, T. Gemming, T. Pichler, M. Knupfer, M. Kalbac, L. Dunsch, O. Jost, S. R. P. Silva, W. Pompe, and B. Buchner, *Nano Lett.* 5, 1209 **(2005)**.

91. S. Han, X. Liu, and C. Zhou, *J. Am. Chem. Soc.* 127, 5294 **(2005)**.

92. D. Takagi, H. Hibino, S. Suzuki, Y. Kobayashi, and Y. Homma, *Nano Lett.* 7, 2272 **(2007)**.

93. M. Kusunoki, T. Suzuki, T. Hirayama, and N. Shibata, *Appl. Phys. Lett.* 77, 531 **(2000)**.

94. E. J. Bae, W. B. Choi, K. S. Jeong, J. U. Chu, G. S. Park, S. Song, and Y. U. Yoo, *Adv. Mater.* 14, 277 **(2002)**.

95. J. J. Schneider, N. I. Maksimova, J. Engstler, R. Joshi, R. Schierholz, and R. Feile, *Inorg. Chim. Acta* 361, 1770 **(2008)**.

96. W. Merchan-Merchan, A. Savaliev, L. A. Kennedy, and A. Fridman, *Chem. Phys. Lett.* 354, 20 **(2002)**.

97. M. H. Rummeli, C. Kramberger, A. Gruneis, P. Ayala, T. Gemming, B. Buchner, and T. Pichler, *Chem. Mater.* 19, 4105 **(2007)**.

98. M. H. Rummeli, F. Schaffel, C. Kramberger, T. Gemming, A. Bachmatiuk, R. J. Kalenczuk, B. Rellinghaus, B. Buchner, and T. Pichler, *J. Am. Chem. Soc.* 129, 15772 **(2007)**.

99. B. Liu, W. Ren, L. Gao, S. Li, S. Pei, C. Liu, C. Jiang, and H. M. Cheng, *J. Am. Chem. Soc.* 131, 2082 **(2009)**.

100. H. Liu, D. Takagi, S. Chiashi, and Y. Homma, *Carbon* 48, 114 **(2010)**.

101. S. Huang, Q. Cai, J. Chen, Y. Qian, and L. Zhang, *J. Am. Chem. Soc.* 131, 2094 **(2009)**.

102. S. Reich, L. Li, and J. Robertson, *Chem. Phys. Lett.* 421, 469 **(2006)**.

103. R. V. Parthasarathy, K. L. N. Phani, and C. R. Martin, *Adv. Mater.* 7, 896 **(1995)**.

104. T. Kyotani, L. F. Tsai, and A. Tomita, *Chem. Mater.* 8, 2109 **(1996)**.

105. C. Y. Han, Z. L. Xiao, H. H. Wang, X. M. Lin, S. Trasobares, and R. E. Cook, *J. Nanomater.* 2009, 562376 **(2009)**.

106. M. Sankaran and B. Viswanathan, *Indian J. Chem.* 47A, 808 **(2008)**.
107. Z. K. Tang, H. D. Sun, J. Wang, J. Chen, and G. Li, *Appl. Phys. Lett.* 73, 2287 **(1998)**.
108. J. Zhai, Z. Tang, P. Sheng, and X. Hu, *IEEE 2006*, ICONN, IEEE, Brisbane, July **(2006)**, p. 155.
109. M. Terrones, N. Grobert, J. Olivares, J. P. Zhang, H. Terrones, K. Kordatos, W. K. Hsu, J. P. Hare, P. D. Townsend, K. Prassides, A. K. Cheetham, H. W. Kroto, and D. R. M. Walton, *Nature* 388, 52 **(1997)**.
110. M. Yudasaka, R. Kikuchi, Y. Ohki, and S. Yoshimura, *Carbon* 35, 195 **(1997)**.
111. B. C. Satishkumar, P. J. Thomas, A. Govindaraj, and C. N. R. Rao, *Appl. Phys. Lett.* 77, 2530 **(2000)**.
112. F. L. Deepak, A. Govindaraj, and C. N. R. Rao, *Chem. Phys. Lett.* 345, 5 **(2001)**.
113. G. Kucukayan, S. Kayacan, B. Baykal, and E. Bengu, *Mater. Res. Soc. Symp. Proc. (Symposium-P)* 1081E, P05 **(2008)**.
114. M. Kumar, X. Zhao, and Y. Ando, *International Symposium on Nanocarbons*, Nagano, Japan, Extended Abstract, November **(2001)**, pp. 244–245.
115. M. Kumar, X. Zhao, Y. Ando, S. Iijima, M. Sharon, and K. Hirahara, *Mol. Cryst. Liq. Cryst.* 387, 117 **(2002)**.
116. M. Kumar and Y. Ando, *Diamond Related Mater.* 12, 998 **(2003)**.
117. M. Kumar and Y. Ando, *Diamond Related Mater.* 12, 1845 **(2003)**.
118. M. Kumar, T. Okazaki, M. Hiramatsu, and Y. Ando, *Carbon* 45, 1899 **(2007)**.
119. M. Kumar and Y. Ando, *Defence Sci. Journal* 58, 496 **(2008)**.
120. M. Sharon, W. K. Hsu, H. W. Kroto, D. R. M. Walton, A. Kawahara, T. Ishihara, and Y. Takita, *J. Power Sources* 104, 148 **(2002)**.
121. R. J. Andrews, C. F. Smith, and A. J. Alexander, *Carbon* 44, 341 **(2006)**.
122. K. Yamada, K. Abe, M. Mikami, M. Saito, and J. Kuwano, *Key Engg. Mater.* 320, 163 **(2006)**.
123. S. P. Somani, P. R. Somani, A. Yoshida, M. Tanemura, S. P. Lau, and M. Umeno, *Solid-State Electron.* 52, 1015 **(2008)**.
124. S. P. Somani, P. R. Somani, M. Tanemura, S. P. Lau, and M. Umeno, *Current Appl. Phys.* 9, 144 **(2009)**.
125. H. Parshotam, M. Tech. Thesis, Chem. Dept., University of Johannesburg **(2008)**.
126. E. F. Antunes, E. C. Almeida, C. B. F. Rosa, L. I. de Medeiros, L. C. Pardini, M. Massi, and E. J. Corat, *J. Nanosci. Nanotechnol.* 10 **(2010)**, doi:10.1166/jnn.2010.1830, in press.
127. J. Tang, G. Jin, Y. Wang, and X Guo, *Carbon* 48, 1545 **(2010)**.
128. S. Musso, G. Fanchini, and A. Tagliaferro, *Diamond Related Mater.* 14, 784 **(2005)**.
129. S. Porro, S. Musso, M. Giorcelli, A. Tagliaferro, S. H. Dalal, K. B. K. Teo, D. A. Jefferson, and W. I. Milne, *J. Non-Cryst. Solids* 352, 1310 **(2006)**.
130. S. Musso, S. Porro, M. Giorcelli, M. Giorrcelli, A. Chiodoni, A. C. Ricciardi, and A. Tagliaferro, *Carbon* 45, 1133 **(2007)**.
131. S. Musso, S. Porro, M. Rovere, M. Giorcelli, and A. Tagliaferro, *J. Cryst. Growth* 310, 477 **(2008)**.
132. M. Pavese, S. Musso, S. Bianco, M. Giorcelli, and N. Pugno, *J. Phys. Condens. Matter.* 20, 474206 **(2008)**.
133. S. Bianco, M. Giorcelli, S. Musso, M. Castellino, F. Agresti, A. Khandelwal, S. L. Russo, M. Kumar, and Y. Ando, *J. Nanosci. Nanotechnol.* 9, 6806 **(2009)**.
134. M. Sharon and M. Sharon, *Synth. React. Inorg. Met.-Org. Nano-Metal. Chem.* 36, 265 **(2006)**.
135. A. K. Chatterjee, M. Sharon, R. Banerjee, and M. Neumann-Spallart, *Electrochim. Acta* 48, 3439 **(2003)**.
136. R. A. Afre, T. Soga, T. Jimbo, M. Kumar, Y. Ando, and M. Sharon, *Chem. Phys. Lett.* 414, 6 **(2005)**.
137. R. A. Afre, T. Soga, T. Jimbo, M. Kumar, Y. Ando, M. Sharon, P. R. Somani, and M. Umeno, *Microporous Mesoporous Mater.* 96, 184 **(2006)**.
138. P. Ghosh, T. Soga, M. Tanemura, M. Zamri, T. Jimbo, R. Katoh, and K. Sumiyama, *Appl. Phys. A* 94, 51 **(2009)**.
139. D. Pradhan and M. Sharon, *Mater. Sci. Engg. B* 96, 24 **(2002)**.
140. J. Qiu, Q. Li, Z. Wang, Y. Sun, and H. Zhang, *Carbon* 44, 2565 **(2006)**.
141. W. Qian, H. Yu, F. Wei, Q. Zhang, and Z. Wang, *Carbon* 40, 2968 **(2002)**.
142. Z. Kang, E. Wang, B. Mao, Z. Su, L. Chen, and L. Xu, *Nanotechnology* 16, 1192 **(2005)**.
143. W. Z. Li, J. G. Wen, and Z. F. Ren, *Appl. Phys. A* 74, 397 **(2002)**.
144. W. Z. Li, J. G. Wen, Y. Tu, and Z. F. Ren. *Appl. Phys. A* 73, 259 **(2001)**.
145. S. Maruyama, Y. Murakami, Y. Shibata, Y. Miyauchi, and S. Chiashi, *J. Nanosci. Nanotechnol.* 4, 360 **(2004)**.
146. J. Li, C. Papadopoulos, J. M. Xu, and M. Moskovits, *Appl. Phys. Lett.* 75, 367 **(1999)**.
147. C. Bower, O. Zhou, W. Zhu, D. J. Werder, and S. Jin, *Appl. Phys. Lett.* 77, 2767 **(2000)**.
148. G. G. Tibbetts, *J. Cryst. Growth* 66, 632 **(1984)**.
149. R. S. Wagner and W. C. Ellis, *Trans. Metallurg. Soc. AIME* 233, 1053 **(1965)**.
150. F. Ding, K. Bolton, and A. Rosen, *J. Chem. Phys. B* 108, 17369 **(2004)**.
151. A. R. Harutyunyan and T. Tokune, *Appl. Phys. Lett.* 87, 051919 **(2005)**.
152. F. Ding, K. Bolton, and A. Rosen, *Comput. Mater. Sci.* 35, 243 **(2006)**.
153. S. Helveg, C. Lopez-Cartes, J. Sehested, P. L. Hansen, B. S. Clausen, J. R. Rostrup-Nielsen, F. Abild-Pedersen, and J. K. Nørskov, *Nature* 427, 426 **(2004)**.
154. J. Y. Raty, F. Gygi, and G. Galli, *Phys. Rev. Lett.* 95, 096103 **(2005)**.
155. S. Hofmann, R. Sharma, C. Ducati, G. Du, C. Mattevi, C. Cepek, M. Cantoro, S. Pisana, A. Parvez, F. Cervantes-Sodi, A. C. Ferrari, R. Dunin-Borkowski, S. Lizzit, L. Petaccia, A. Goldoni, and J. Robertson, *Nano Lett.* 7, 602 **(2007)**.
156. J. A. Rodriguez-Manzo, M. Terrones, H. Terrones, H. W. Kroto, L. Sun, and F. Banhart, *Nat. Nanotechnol.* 2, 307 **(2007)**.
157. M. S. Kim, N. M. Rodriguez, and R. T. K. Baker, *J. Catal.* 134, 253 **(1992)**.
158. P. E. Nolan, D. C. Lynch, and A. H. Cutler, *J. Phys. Chem. B* 102, 4165 **(1998)**.
159. R. T. K. Baker, J. R. Alonzo, J. A. Dumesic, and D. J. C. Yates, *J. Catal.* 77, 74 **(1982)**.
160. K. L. Yang and R. T. Yang, *Carbon* 24, 687 **(1986)**.
161. M. Audier, P. Bowen, and W. Jones, *J. Cryst. Growth* 64, 291 **(1983)**.
162. C. Ducati, I. Alexandrou, M. Chhowalla, J. Robertson, and G. A. J. Amaratunga, *J. Appl. Phys.* 95, 6387 **(2004)**.
163. H. Yoshida, S. Takeda, T. Uchiyama, H. Kohno, and Y. Homma, *Nano Lett.* 8, 2082 **(2008)**.
164. C. T. Wirth, S. Hofmann, and J. Robertson, *Diamond Related Mater.* 18, 940 **(2009)**.
165. M. J. Bronikowski, P. A. Willis, D. T. Colbert, K. A. Smith, and R. E. Smalley, *J. Vac. Sci. Technol. A* 19, 1800 **(2001)**.
166. WTEC Study Report on International Assessment of Research and Development of Carbon Nanotube Manufacturing and Applications, World Technology Evaluation Center Inc., USA **(2007)**.
167. A. M. Cassell, J. A. Raymakers, J. Kong, and H. Dai, *J. Phys. Chem. B* 103, 6484 **(1999)**.
168. M. Endo, T. Hayashi, Y. A. Kim, and H. Muramatsu, *Jpn. J. Appl. Phys.* 45, 4883 **(2006)**.
169. Q. Zhang, M. Zhao, J. Huang, J. Nie, and F. Wei, *Carbon* 48, 1196 **(2010)**.

170. L. A. Montoro, P. Corio, and J. M. Rosolen, *Carbon* 45, 1234 **(2007)**.
171. S. Musso, M. Zanetti, M. Giorcelli, A. Tagliaferro, and L. Costa, *J. Nanosci. Nanotecnol.* 9, 3593 **(2009)**.
172. N. Das, A. Dalai, J. S. S. Mohammadzadeh, and J. Adjaye, *Carbon* 44, 2236 **(2006)**.
173. Y. Tian, Z. Hu, Y. Yang, X. Wang, X. Chen, and H. Xu, *J. Am. Chem. Soc*. 126, 1180 **(2004)**.
174. P. Anastas and J. C. Warner, Green Chemistry: Theory and Practice, Oxford University Press, Oxford **(1998)**, p. 30.
175. M. J. Eckelman, J. B. Zimmerman, and P. T. Anastas, *J. Industrial Ecology* 12, 316 **(2008)**.
176. S. M. Bachilo, L. Balzano, J. E. Herrera, F. Pompeo, D. E. Resasco, and R. B. Weisman, *J. Am. Chem. Soc*. 125, 11186 **(2003)**.
177. V. López, L. Welte, M. A. Fernández, M. Moreno-Moreno, J. Gómez-Herrero, P. J. de Pablo, and F. Zamora, *J. Nanosci. Nanotechnol.* 9, 2830 **(2009)**.
178. Y. Wang, M. J. Kim, H. Shan, C. Kittrell, H. Fan, L. M. Ericson, W. F. Hwang, S. Arepalli, R. H. Hauge, and R. E. Smalley, *Nano Lett.* 5, 997 **(2005)**.
179. H. J. Jeong, K. K. Kim, S. Y. Jeong, M. H. Park, C. W. Yang, and Y. H. Lee, *J. Phys. Chem. B* 108, 17695 **(2004)**.
180. K. Y. Chun, S. Jung, H. Y. Choi, J. U. Kim, and C. J. Lee, *J. Nanosci. Nanotechnol.* 9, 2148 **(2009)**.
181. N. Bajwa, X. Li, P. M. Ajayan, and R. Vajtai, *J. Nanosci. Nanotechnol.* 8, 6054 **(2008)**.
182. C. T. Wirth, C. Zhang, G. Zhong, S. Hofmann, and J. Robertson, *ACS Nano.* 3, 3560 **(2009)**.
183. P. B. Amama, C. L. Pint, L. McJilton, S. M. Kim, E. A. Stach, P. T. Murray, R. H. Hauge, and B. Maruyama, *Nano Lett.* 9, 44 **(2009)**.
184. T. Maruyama, K. Sato, Y. Mizutani, K. Tanioku, T. Shiraiwa, and S. Naritsuka, *J. Nanosci. Nanotechnol.* 10, 4095 **(2010)**.
185. A. R. Harutyunyan, *J. Nanosci. Nanotechnol.* 9, 2480 **(2009)**.

Received: 29 January 2010. Revised/Accepted: 1 February 2010.